CANCER

Lectin-type oxidized LDL receptor-1 distinguishes population of human polymorphonuclear myeloid-derived suppressor cells in cancer patients

Thomas Condamine,[1]* George A. Dominguez,[1] Je-In Youn,[1†] Andrew V. Kossenkov,[1] Sridevi Mony,[1] Kevin Alicea-Torres,[1] Evgenii Tcyganov,[1] Ayumi Hashimoto,[1] Yulia Nefedova,[1] Cindy Lin,[1] Simona Partlova,[1‡] Alfred Garfall,[2,3] Dan T. Vogl,[2,3] Xiaowei Xu,[2] Stella C. Knight,[4] George Malietzis,[4,5] Gui Han Lee,[4,5] Evgeniy Eruslanov,[2] Steven M. Albelda,[2,3] Xianwei Wang,[6] Jawahar L. Mehta,[6] Meenakshi Bewtra,[3] Anil Rustgi,[2,3] Neil Hockstein,[7] Robert Witt,[7] Gregory Masters,[7] Brian Nam,[7] Denis Smirnov,[8] Manuel A. Sepulveda,[8] Dmitry I. Gabrilovich[1§]

Polymorphonuclear myeloid-derived suppressor cells (PMN-MDSCs) are important regulators of immune responses in cancer and have been directly implicated in the promotion of tumor progression. However, the heterogeneity of these cells and the lack of distinct markers hamper the progress in understanding the biology and clinical importance of these cells. Using partial enrichment of PMN-MDSC with gradient centrifugation, we determined that low-density PMN-MDSC and high-density neutrophils from the same cancer patients had a distinct gene profile. The most prominent changes were observed in the expression of genes associated with endoplasmic reticulum (ER) stress. Unexpectedly, low-density lipoprotein (LDL) was one of the most increased regulators, and its receptor oxidized LDL receptor 1 (*OLR1*) was one of the most overexpressed genes in PMN-MDSC. Lectin-type oxidized LDL receptor-1 (LOX-1) encoded by *OLR1* was practically undetectable in neutrophils in peripheral blood of healthy donors, whereas 5 to 15% of total neutrophils in cancer patients and 15 to 50% of neutrophils in tumor tissues were LOX-1$^+$. In contrast to their LOX-1$^-$ counterparts, LOX-1$^+$ neutrophils had gene signature, potent immunosuppressive activity, up-regulation of ER stress, and other biochemical characteristics of PMN-MDSCs. Moreover, induction of ER stress in neutrophils from healthy donors up-regulated LOX-1 expression and converted these cells to suppressive PMN-MDSCs. Thus, we identified a specific marker of human PMN-MDSC associated with ER stress and lipid metabolism, which provides new insights into the biology and potential therapeutic targeting of these cells.

INTRODUCTION

The accumulation of relatively immature and pathologically activated myeloid-derived suppressor cells (MDSCs) with potent immunosuppressive activity is common in tumors. MDSCs have the ability to support tumor progression by promoting tumor cell survival, angiogenesis, invasion of healthy tissue by tumor cells, and metastases [reviewed in (*1*)]. There is now ample evidence of the association of accumulation of immunosuppressive MDSCs with negative clinical outcomes in various cancers (*2*). MDSCs have been implicated in resistance to anticancer therapies with kinase inhibitor (*3*), chemotherapy (*4*–*7*), and immunotherapy (*8*–*12*).

Two large populations of MDSCs are currently described: polymorphonuclear MDSCs (PMN-MDSCs) and monocytic MDSCs (M-MDSCs) (*13*). PMN-MDSC is the most abundant population of MDSC in most types of cancer, phenotypically and morphologically similar to neutrophils (PMNs) (*14*). These cells share the CD11b$^+$CD14$^-$CD15$^+$/CD66b$^+$ phenotype. At present, these cells can be separated only in peripheral blood (PB) and only by density gradient centrifugation. Distinction between PMN-MDSC and PMN in tumor tissues is not possible. Because gradient centrifugation may enrich not only for true PMN-MDSC but also for activated PMN without suppressive activity, the heterogeneity of PMN-MDSC population raised the questions of whether PMN-MDSC and PMN are truly cells with distinct features. It is not clear what defines the specific functional state of human PMN-MDSC vis-à-vis PMN in the same patient. The mechanisms responsible for the acquisition of pathological activity by human neutrophils in cancer remained unclear.

Here, we attempted to address these questions by evaluating populations of PMN-MDSC and PMN from the same patients. We identified genomic signature of PMN-MDSCs and surface markers specific for these cells. We found that induction of endoplasmic reticulum (ER) stress response was sufficient to convert neutrophils to PMN-MDSCs.

RESULTS

Human PMN-MDSCs have a distinct gene expression profile from neutrophils

To compare PMN-MDSC and PMN from PB of the same patients with non–small cell lung cancer (NSCLC) and head and neck cancer (HNC), we used dual-density Histopaque gradient, the standard method of isolation of PMN-MDSC (*15*). Low-density PMN-MDSCs are copurified

[1]Wistar Institute, Philadelphia, PA 19104, USA. [2]Abramson Cancer Center, University of Pennsylvania, Philadelphia, PA 19104, USA. [3]Department of Medicine, Perelman School of Medicine, University of Pennsylvania, Philadelphia, PA 19104, USA. [4]Antigen Presentation Research Group, Imperial College London, London HA1 3UJ, UK. [5]St. Mark's Hospital, Harrow HA1 3UJ, UK. [6]Department of Medicine, University of Arkansas for Medical Sciences, Little Rock, AR 72205, USA. [7]Helen F. Graham Cancer Center & Research Institute, Christiana Care Health System, Newark, DE 19713, USA. [8]Janssen Oncology Therapeutic Area, Janssen Research and Development LLC, Pharmaceutical Companies of Johnson & Johnson, Spring House, PA 19477, USA.
*Present address: Incyte Corporation, 1801 Augustine Cut-Off, Wilmington, DE 19803, USA.
†Present address: Wide River Institute of Immunology, Department of Biomedical Sciences, Seoul National University College of Medicine, Seoul 03080, South Korea.
‡Present address: SOTIO a.s., Prague, Czech Republic.
§Corresponding author. Email: dgabrilovich@wistar.org

with peripheral blood mononuclear cells (PBMCs), whereas high-density PMNs are collected from lower gradient (*16*). As a control, PMNs from healthy donors were used. Both low-density PMN-MDSCs and high-density PMNs were purified further with CD15 magnetic beads to achieve similar high purity of both cell populations (Fig. 1A). The immunosuppressive activity of PMN-MDSC, the main characteristic of these cells, was confirmed in allogeneic mixed leukocyte reaction (MLR) (Fig. 1B) and in autologous system with T cells activated by CD3/CD28 antibodies (Fig. 1C). As expected, PMNs were not suppressive (Fig. 1, B and C).

To study overall differences and similarities between patients' PMNs and PMN-MDSCs as well as PMNs from healthy donors, we performed whole-genome analysis using Illumina HumanHT-12 v4 bead arrays. The direct pairwise comparison identified 1870 array probes significantly differentially expressed [false discovery rate (FDR) < 5%] between PMN-MDSC and PMN in the same patients (fig. S1A), and 36 probes showed difference of at least fivefold (fig. S1B). Hierarchical clustering of the samples using expression of the 985 most differentially expressed genes (fold > 2, $P < 0.05$; Fig. 1D) revealed that PMN-MDSC samples have a unique expression profile and PMNs from cancer patients are very similar to healthy donor PMN samples, because they grouped within the same cluster for HNC and NSCLC patients (Fig. 1E). Specifically, of the 985 genes that were different between any pair of groups, most (74%) showed significant differences (FDR < 5%) between patients' PMN-MDSCs and PMNs, whereas no genes were significantly different when corrected for multiple testing (best FDR = 19%) between PMNs from healthy donors and PMNs from cancer patients, with only 12% of the genes significantly different at nominal $P < 0.05$, which indicates a high similarity of PMN samples between cancer patients and healthy donors.

Using Ingenuity Pathway Analysis (IPA), we identified 14 pathways significantly enriched in PMN-MDSCs, including eukaryotic translation initiation factor 2 (eIF2) and eIF4 pathways and mechanistic target of rapamycin signaling (table S1). The regulators of genes enriched in PMN-MDSC included regulators of ER stress response, mitogen-activated protein kinase pathway, colony-stimulating factor 1 (CSF1), interleukin-6 (IL-6), interferon-γ, and nuclear factor-κB (NF-κB). These molecules were previously directly implicated in MDSC biology, primarily PMN-MDSC [reviewed in (*17*)]. One of the most significant changes was associated with low-density lipoprotein (LDL) (Fig. 1F). Thus, PMN-MDSCs had a distinct genomic profile from PMNs isolated from the same cancer patients and PMNs from healthy donors. Genes associated with ER stress and immune responses were among the most up-regulated in PMN-MDSC.

LOX-1 is differentially expressed in PMN-MDSC and PMN

To search for potential markers of PMN-MDSCs, we evaluated differentially expressed genes, which encoded surface molecules, and compared the expression of various surface molecules between PMN-MDSCs and PMNs from the same patients and PMNs from healthy donors. More than 20 genes that encoded surface molecules were found to be differentially expressed in PMN-MDSC and PMN (Fig. 2A). In an attempt to validate these observations, we tested surface expression of some of the proteins using available antibodies and flow cytometry. Unexpectedly, the differences were found in the expression of lectin-type oxidized LDL receptor-1 (LOX-1), a 50-kDa transmembrane glycoprotein encoded by the oxidized LDL receptor 1 (*OLR1*) gene (*18*). In our analysis, *OLR1* was one of the mostly up-regulated genes in PMN-MDSCs (fig. S1B). LOX-1 is one of the main receptors for oxidized LDL (oxLDL) (*19*). It also binds other ligands including other modified lipoproteins, advanced glycation end products, aged red blood cells, apoptotic cells, and activated platelets (*20*). LOX-1 is expressed in endothelial cells, macrophages, smooth muscle cells, and some intestinal cell lines (*18*). However, it was not associated with neutrophils.

We evaluated LOX-1 expression in high-density PMNs and low-density PMN-MDSCs in cancer patients (Fig. 2B). LOX-1 was practically undetectable in PMN but expressed in about one-third of PMN-MDSC fraction (Fig. 2C). Because LOX-1 can be expressed in platelets (*21*) and platelets can adhere to activated PMN, we asked whether the increased expression of LOX-1 in PMN-MDSC fraction was the result of increased adherence of platelets. However, LOX-1$^-$ and LOX-1$^+$ cells in low-density PMN-MDSC population had the same small proportion of cells that express platelet markers CD41a and CD42b (Fig. 2D). We determined whether LOX-1 expression in PMN correlated with CD16 expression associated with neutrophil activation (*22*, *23*). Almost all PMNs in cancer patients were CD16^{hi}, and expression of LOX-1 on PMN was not associated with CD16 expression (fig. S2).

These results suggested that LOX-1 could be associated with PMN-MDSC. We asked whether LOX-1 can be a marker of PMN-MDSC. Cell density as a criterion for separation of PMN-MDSC from PMN has serious limitations. It may be changed during handling of cells. In addition, gradient centrifugation may enrich not only for PMN-MDSC but also for activated PMN without suppressive activity, which contributes to well-established heterogeneity of PMN-MDSC population. Therefore, we avoided the use of gradient centrifugation and labeled cells in PB directly with granulocyte-specific CD15 antibody and evaluated the expression of LOX-1 among all CD15$^+$ cells (Fig. 2E). In preliminary experiments, we found no differences in the results obtained with CD15 or CD66b antibodies. We referred to CD15$^+$ cells as PMNs because Siglec-8$^+$ eosinophils represented a very small proportion of CD15$^+$ cells, and no differences in the presence of eosinophils between CD15$^+$LOX-1$^+$ and CD15$^+$LOX-1$^-$ cells were seen (fig. S3). The proportion of LOX-1$^+$ cells among all PMN in healthy donors was very low (range, 0.1 to 1.5; mean, 0.7%) (Fig. 2F and fig. S4). In patients with NSCLC, it increased to 4.9% ($P < 0.001$), in patients with HNC to 6.4% ($P < 0.0001$), and in patients with colon cancer (CC) to 6.5% ($P = 0.0035$) (Fig. 2F). In all three types of cancer, >75% of patients had proportion of LOX-1$^+$ PMN higher than the range established for healthy donors. We also assessed the changes in LOX-1$^+$ PMNs in tumor-free patients with inflammatory conditions: eosinophilic esophagitis, ulcerative colitis, and Crohn's disease. Only patients with Crohn's disease had a small increase in the proportion of these cells (Fig. 2G). Thus, LOX-1 expression defined distinct population of neutrophils in cancer patients and was associated with accumulation of PMN-MDSC.

LOX-1 defines the population of PMN-MDSC among neutrophils

We addressed the question whether LOX-1 can be considered as a marker of human PMN-MDSC. LOX-1$^+$ and LOX-1$^-$ PMNs were sorted directly from PB of the same patients. LOX-1$^-$ PMN had the typical morphology of mature neutrophils, whereas LOX-1$^+$ PMN displayed more immature morphology with band-shaped nuclei (Fig. 3A). Whole-gene expression array was performed on LOX-1$^+$ and LOX-1$^-$ PMNs and compared with that of PMNs and PMN-MDSCs. Analysis of gene expression revealed 639 genes significantly different between LOX-1$^+$ and LOX-1$^-$ (FDR < 5%, fold > 2), and on the basis of the expression of those genes, LOX-1$^+$ PMNs clustered together with PMN-MDSCs, whereas LOX-1$^-$ PMNs were very similar to patients'

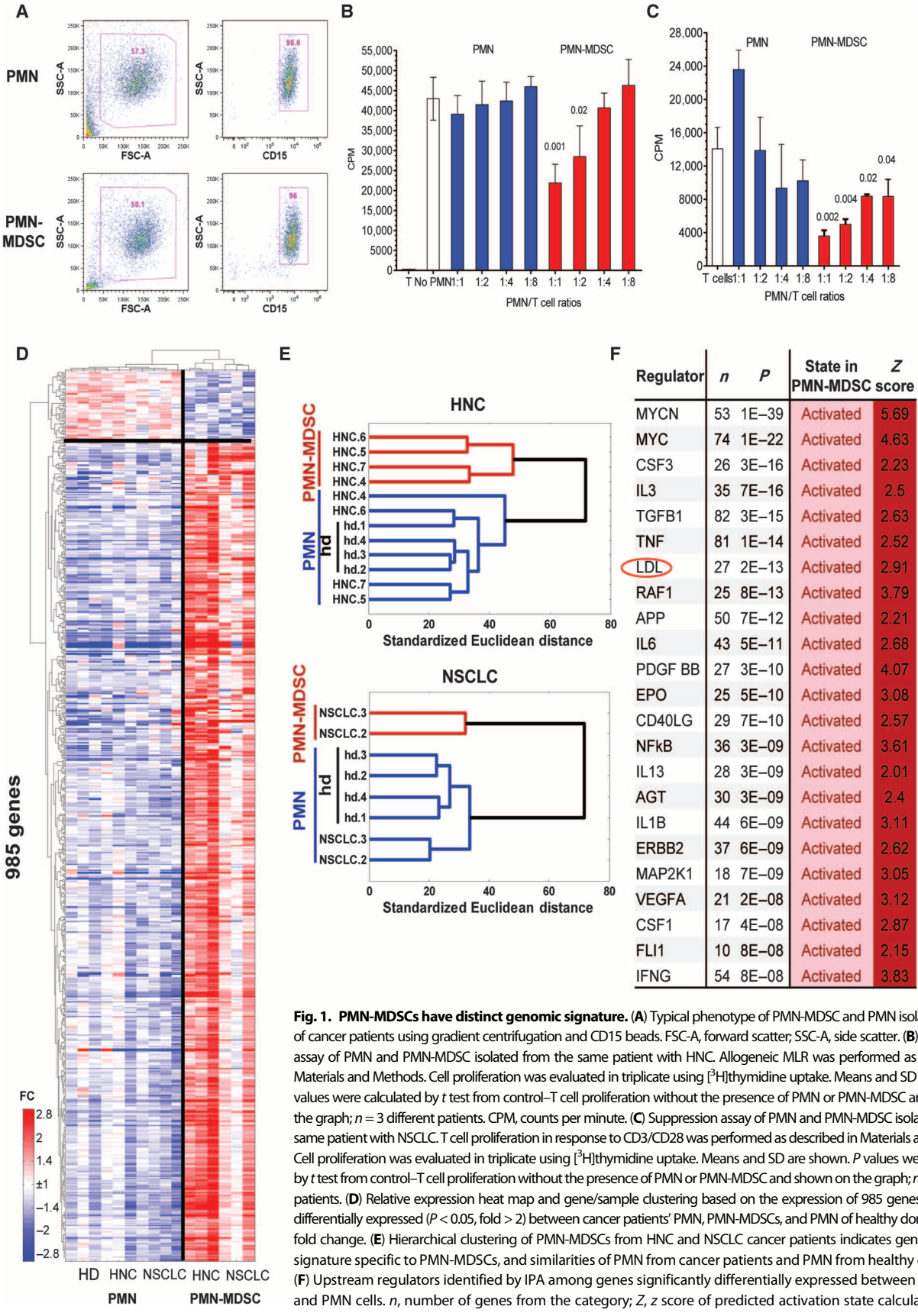

F

Regulator	n	P	State in PMN-MDSC	Z score
MYCN	53	1E–39	Activated	5.69
MYC	74	1E–22	Activated	4.63
CSF3	26	3E–16	Activated	2.23
IL3	35	7E–16	Activated	2.5
TGFB1	82	3E–15	Activated	2.63
TNF	81	1E–14	Activated	2.52
LDL	27	2E–13	Activated	2.91
RAF1	25	8E–13	Activated	3.79
APP	50	7E–12	Activated	2.21
IL6	43	5E–11	Activated	2.68
PDGF BB	27	3E–10	Activated	4.07
EPO	25	5E–10	Activated	3.08
CD40LG	29	7E–10	Activated	2.57
NFkB	36	3E–09	Activated	3.61
IL13	28	3E–09	Activated	2.01
AGT	30	3E–09	Activated	2.4
IL1B	44	6E–09	Activated	3.11
ERBB2	37	6E–09	Activated	2.62
MAP2K1	18	7E–09	Activated	3.05
VEGFA	21	2E–08	Activated	3.12
CSF1	17	4E–08	Activated	2.87
FLI1	10	8E–08	Activated	2.15
IFNG	54	8E–08	Activated	3.83

Fig. 1. PMN-MDSCs have distinct genomic signature. (**A**) Typical phenotype of PMN-MDSC and PMN isolated from PB of cancer patients using gradient centrifugation and CD15 beads. FSC-A, forward scatter; SSC-A, side scatter. (**B**) Suppression assay of PMN and PMN-MDSC isolated from the same patient with HNC. Allogeneic MLR was performed as described in Materials and Methods. Cell proliferation was evaluated in triplicate using [^{3}H]thymidine uptake. Means and SD are shown. *P* values were calculated by *t* test from control–T cell proliferation without the presence of PMN or PMN-MDSC and shown on the graph; $n = 3$ different patients. CPM, counts per minute. (**C**) Suppression assay of PMN and PMN-MDSC isolated from the same patient with NSCLC. T cell proliferation in response to CD3/CD28 was performed as described in Materials and Methods. Cell proliferation was evaluated in triplicate using [^{3}H]thymidine uptake. Means and SD are shown. *P* values were calculated by *t* test from control–T cell proliferation without the presence of PMN or PMN-MDSC and shown on the graph; $n = 3$ different patients. (**D**) Relative expression heat map and gene/sample clustering based on the expression of 985 genes significantly differentially expressed ($P < 0.05$, fold > 2) between cancer patients' PMN, PMN-MDSCs, and PMN of healthy donors (HD). FC, fold change. (**E**) Hierarchical clustering of PMN-MDSCs from HNC and NSCLC cancer patients indicates gene expression signature specific to PMN-MDSCs, and similarities of PMN from cancer patients and PMN from healthy donors (hd). (**F**) Upstream regulators identified by IPA among genes significantly differentially expressed between PMN-MDSC and PMN cells. *n*, number of genes from the category; *Z*, *z* score of predicted activation state calculated by IPA.

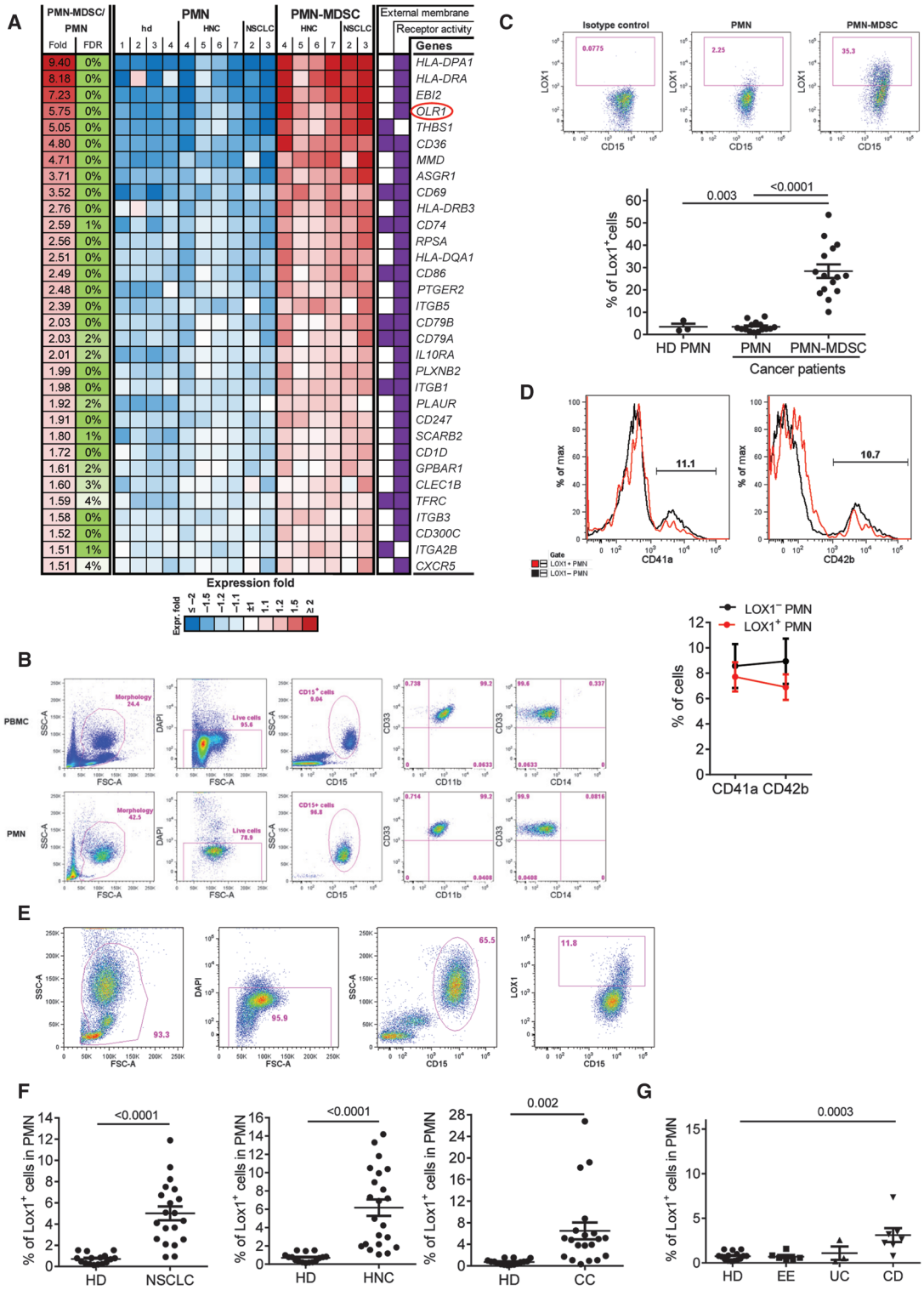

Fig. 2. LOX-1 as a marker of PMN-MDSC. (**A**) List and a heat map of relative expression of candidate surface markers specific to the PMN-MDSCs. (**B**) Typical phenotype of high-density PMN and low-density PMN-MDSC in a cancer patient. (**C**) Proportion of LOX-1$^+$ PMN and PMN-MDSC in PB of 15 cancer patients. (Top) Example of staining of PMN-MDSC and PMN with LOX-1 antibody. Cells were isolated using density gradient as described in Materials and Methods, and the proportion of LOX-1$^+$ cells was calculated among CD15$^+$ cells. (Bottom) Individual results for each patient are means and SE. *P* values (*t* test) are shown. (**D**) Example of staining with CD41a and CD42b antibody (top). Cumulative results of seven patients with NSCLC (bottom). Means and SD are shown. (**E**) Typical example of the analysis of PMN in a cancer patient. (**F**) Proportion of LOX-1$^+$ cells among PMN in unseparated PB from 16 healthy donors, 20 patients with NSCLC, 21 patients with HNC, and 19 patients with CC. *P* values calculated by *t* test are shown. (**G**) Proportion of LOX-1$^+$ cells among PMN in unseparated PB from 16 healthy donors, 6 patients with eosinophilic esophagitis (EE), 3 patients with ulcerative colitis (UC), and 7 patients with Crohn's disease (CD). *P* values calculated by *t* test are shown.

and healthy donors' PMNs (Fig. 3B). Overall, 92% of those genes had the same direction of change between LOX-1$^+$ and LOX-1$^-$ as between PMN-MDSCs and PMNs, with 93 probes significantly up-regulated (FDR < 5%) at least twofold or more in both PMN-MDSCs and LOX-1$^+$ PMNs (Fig. 3C and fig. S5). Thus, LOX-1$^+$ PMNs from cancer patients had gene expression profile similar to PMN-MDSCs.

The hallmark of PMN-MDSCs is their ability to suppress T cell function. We isolated LOX-1$^-$ and LOX-1$^+$ PMNs directly from PB of cancer patients and used them in T cell suppression assay. LOX-1$^+$ PMNs suppressed T cell proliferation, whereas LOX-1$^-$ PMNs did not (Fig. 3D). We asked whether the LOX-1 antibody used for isolation of PMN-MDSCs could directly affect the functional activity of PMN. PMNs isolated from cancer patients were cultured with T cells in the presence of LOX-1 antibody or immunoglobulin G (IgG) isotype control. LOX-1 antibody did not make PMNs to acquire immunosuppressive function (fig. S6). We determined whether LOX-1 neutralizing antibody (R&D Systems) could block the suppressive activity of LOX-1$^+$ PMNs. LOX-1$^+$ and LOX-1$^-$ PMNs were isolated from two patients with NSCLC and added to MLR in the presence of LOX-1 antibody at a concentration (10 μg/ml) that blocks more than 90% of LOX-1 binding or the same amount of mouse IgG. In both experiments, LOX-1 antibody did not abrogate the suppressive activity of LOX-1$^+$ PMNs. LOX-1$^-$ PMNs had no suppressive activity in any experiment (Fig. 3E).

We then evaluated possible mechanisms responsible for LOX-1$^+$ PMN-MDSC suppression. We tested several common mechanisms implicated in PMN-MDSC function. LOX-1$^+$ PMN-MDSCs had significantly higher production of reactive oxygen species (ROS) than LOX-1$^-$ PMN (Fig. 3F). Whole-genome array showed that LOX-1$^+$ PMN-MDSCs had higher expression of arginase 1 (*ARG1*), the gene directly associated with PMN-MDSC function, than LOX-1$^-$ PMNs. These differences were not statistically significant (FDR, 7%). However, direct evaluation of *ARG1* expression by quantitative polymerase chain reaction (qPCR) revealed significantly higher expression of this gene in LOX-1$^+$ PMN-MDSCs than in LOX-1$^-$ PMNs (Fig. 3G). The expression of *NOS2* in PMNs was much lower than that of *ARG1*. However, it was still significantly higher in LOX-1$^+$ PMN-MDSCs than in LOX-1$^-$ PMNs (Fig. 3G). We tested the contribution of ROS and ARG1 to immunosuppression mediated by LOX-1$^+$ PMN-MDSC. ROS scavenger *N*-acetylcysteine (NAC) and catalase significantly decreased the suppressive activity of LOX-1$^+$ PMNs (Fig. 4A). An inhibitor of Arg1, N^{ω}-hydroxy-nor-arginine (nor-NOHA), abrogated the suppressive activity of these cells (Fig. 4B). Together, these data thus demonstrate that LOX-1$^+$ PMNs represent a population of PMN- MDSCs. Therefore, for clarity in this study, we further refer to these cells as LOX-1$^+$ PMN-MDSCs.

We investigated the possible role of LOX-1 as a marker of mouse PMN-MDSCs. Similar to human PMNs, CD11b$^+$Ly6C^{lo}Ly6G$^+$ mouse PMNs had very low expression of LOX-1. In contrast to human PMN-MDSCs, spleen, bone marrow (BM), or tumor PMN-MDSCs from mice bearing EL-4 lymphoma or Lewis lung carcinoma (LLC) did not up-regulate LOX-1 expression (fig. S7). To evaluate the possible role of LOX-1 in PMN-MDSC function, we used BM cells from LOX-1 knockout (KO) (*olr1*$^{-/-}$) mice (*24*). Lethally irradiated wild-type (WT) recipients were reconstituted with congenic BM cells isolated from WT or *olr1*$^{-/-}$ mice. Ten weeks after reconstitution, donor's cells represented more than 95% of all myeloid cells. LLC tumor was implanted subcutaneously, and mice were evaluated 3 weeks later. No differences in the presence of PMN-MDSCs in spleens or tumors were observed between mice reconstituted with WT and LOX-1 KO BM (fig. S8A). WT and *olr1*$^{-/-}$ PMN-MDSCs suppressed T cell proliferation equally well (fig. S8B). Gene expression profile demonstrated no differences between WT and *olr1*$^{-/-}$ PMN-MDSCs. WT PMN-MDSCs had the same undetectable level of *olr1* expression as *olr1*$^{-/-}$ PMN-MDSCs. Thus, in contrast to humans, mouse LOX-1 is not associated with PMN-MDSC.

ER stress regulates LOX-1 expression in PMN-MDSC

What could induce LOX-1 up-regulation in PMN-MDSC? On the basis of the fact that in endothelial cells LOX-1 can be induced by proinflammatory cytokines (*25*), we tested the effect of several cytokines and tumor cell–conditioned medium (TCM) on LOX-1 expression in PMN isolated from healthy donors. None of the tested proinflammatory cytokines [IL-1β, TNF-α (tumor necrosis factor–α), and IL-6] or TCM-induced up-regulation of LOX-1 in PMN after 24-hour culture [granulocyte-macrophage (GM)–CSF] was added to protect PMN viability (Fig. 4C).

Our previous observations (*16*) and data obtained in this study demonstrated that PMN-MDSC in cancer patients displayed signs of ER stress response. LOX-1$^+$ and LOX-1$^-$ PMNs were isolated from PB of cancer patients, and the expression of genes associated with ER stress was evaluated. LOX-1$^+$ PMN-MDSCs had significantly higher expression of spliced X-box–binding protein 1 (*sXBP1*) and its target gene *SEC61a* than LOX-1$^-$ PMNs. The expression of *activating transcription factor 4* (*ATF4*) and its target gene *ATF3* was also higher in LOX-1$^+$ PMN-MDSCs. No changes in the expression of CCAAT/enhancer binding protein (*CHOP*) were observed (Fig. 4D). To test the effect of ER stress on the expression of LOX-1, we treated PMNs from healthy donors with ER stress inducers, thapsigargin (THG) or dithiothreitol (DTT), overnight in the presence of GM-CSF. At selected doses (1 μM THG or 1 mM DTT), cell viability remained above 95%. Both THG and DTT caused marked up-regulation of LOX-1 expression in PMN (Fig. 4E).

Overnight THG treatment of PMNs caused acquisition of potent immunosuppressive activity by the PMNs (Fig. 5A). Because LOX-1$^+$ PMN-MDSCs have increased expression preferentially of one of the ER stress sensors, sXBP1, we verified the role of ER stress using recently developed selective inhibitor of sXBP1, B-I09 (*26*). In the presence of B-I09, THG failed to induce up-regulation of LOX-1 (Fig. 5B) and immunosuppressive activity of PMN (Fig. 5C). THG treatment did not affect typical polymorphonuclear morphology of these cells (Fig. 5D). Thus, induction of ER stress in control neutrophils converted these cells to immunosuppressive PMN-MDSCs, which were associated with up-regulation of LOX-1 expression.

Up-regulation of intracellular Ca^{2+} and ROS is one of the consequences of THG treatment. We asked whether activation of neutrophils with agents that cause up-regulation of intracellular Ca^{2+} and ROS may also result to similar up-regulation of LOX-1 and suppressive activity as THG. We used two compounds: *N*-formyl-Met-Leu-Phe (*f*MLP) and phorbol 12-myristate 13-acetate (PMA). Both *f*MLP and PMA caused massive up-regulation of LOX-1 expression in control PMN within 60 min after the start of the treatment (Fig. 5E). However, in contrast to THG, the expression of LOX-1 in *f*MLP-treated PMN returned to control (untreated cells) level after overnight culture despite the presence of *f*MLP in the culture (Fig. 5E). PMNs did not survive overnight treatment with PMA. PMNs treated for 60 min with *f*MLP or PMA were washed and used in a T cell suppression assay. No suppressive activity was observed (Fig. 5F). In another set of experiments, PMNs were cultured with *f*MLP for 18 hours before they were used in the suppressive assay. However, this treatment did not result in the development of suppressive activity by PMNs (Fig. 5F). These data indicate that transient up-regulation of LOX-1 as a result of PMN activation was not associated with immunosuppressive activity.

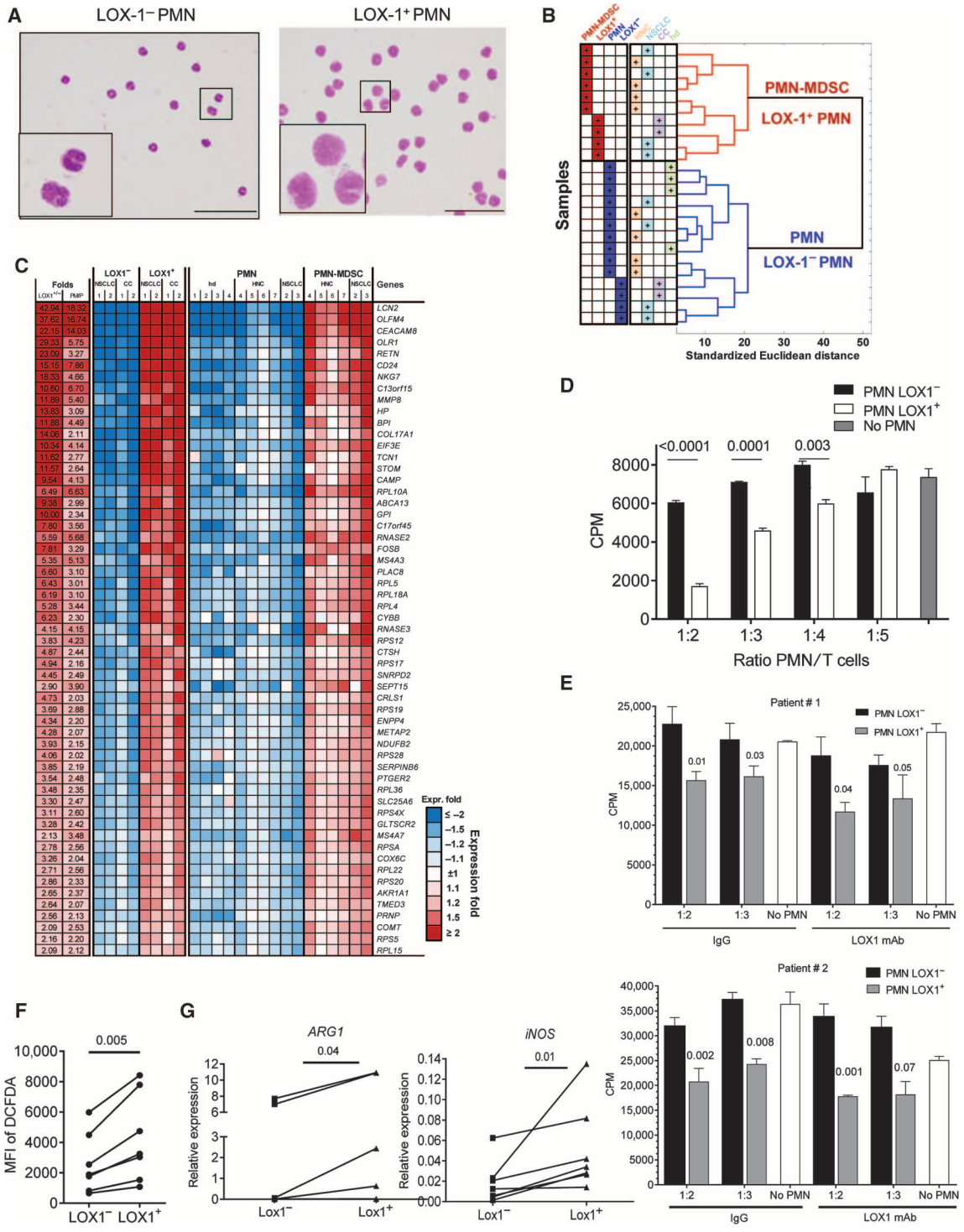

Fig. 3. LOX-1 expression defines bona fide PMN-MDSC. (**A**) Typical morphology of sorted LOX-1$^+$ and Lox-1$^-$ PMN from a patient with HNC. Scale bars, 20 μm. (**B**) Hierarchical clustering of samples based on the expression levels of genes differentially expressed between LOX-1$^+$ and LOX-1$^-$ PMN. (**C**) List and relative expression values of the most changed known genes overlapped between LOX-1$^+$ and PMN-MDSC cells. (**D**) Suppressive activity of LOX-1$^+$ and LOX-1$^-$ PMN isolated from PB of patient with HNC in allogeneic MLR. Cell proliferation was evaluated in triplicate using [^{3}H]thymidine uptake. Means and SE are shown. *P* values calculated by *t* test from T cell proliferation without the presence of PMN are shown. Experiments with similar results were performed with samples from nine patients with HNC and NSCLC. (**E**) Effect of neutralizing LOX-1 antibody on the suppressive activity of LOX-1$^+$ PMN. PMNs were isolated from two patients with NSCLC. LOX-1$^+$ and LOX-1$^-$ PMNs were isolated as described in Materials and Methods and then added to allogeneic MLR in the presence of neutralizing mouse anti-human LOX-1 antibody (10 μg/ml) or mouse IgG. Cell proliferation was evaluated in triplicate using [^{3}H]thymidine uptake. Means and SE are shown. *P* values calculated by *t* test from T cell proliferation without the presence of PMN are shown. (**F**) ROS production in LOX-1$^+$ and LOX-1$^-$ PMN from seven patients with HNC and NSCLC. ROS production was measured by staining with 2′,7′-dichlorofluorescin diacetate (DCFDA). MFI, mean fluorescence intensity. (**G**) Expression of *ARG1* and *NOS2* in LOX-1$^+$ and LOX-1$^-$ PMN from six patients with HNC and MM measured by qPCR. *P* values calculated by *t* test are shown.

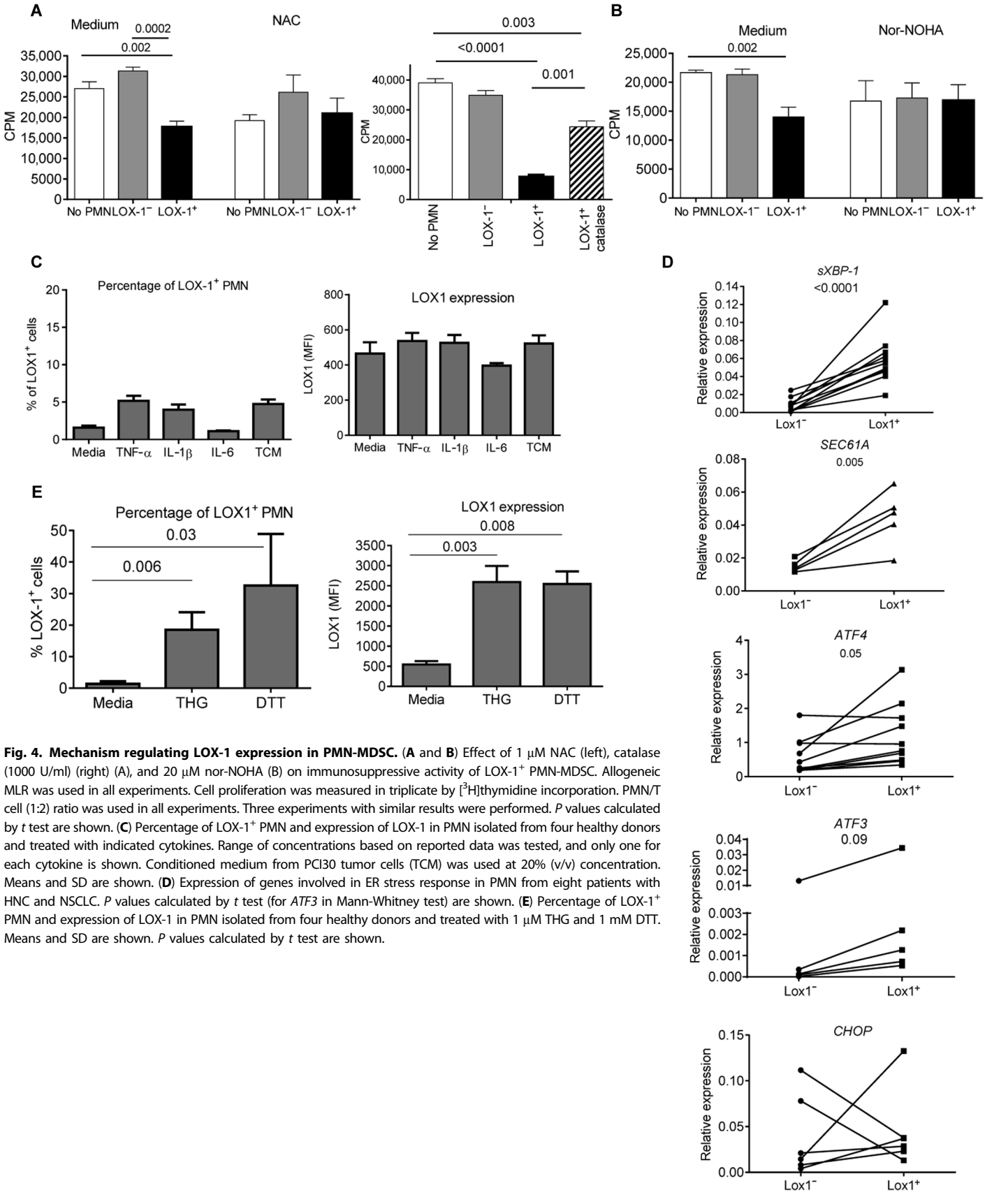

Fig. 4. Mechanism regulating LOX-1 expression in PMN-MDSC. (**A** and **B**) Effect of 1 μM NAC (left), catalase (1000 U/ml) (right) (A), and 20 μM nor-NOHA (B) on immunosuppressive activity of LOX-1$^+$ PMN-MDSC. Allogeneic MLR was used in all experiments. Cell proliferation was measured in triplicate by [^{3}H]thymidine incorporation. PMN/T cell (1:2) ratio was used in all experiments. Three experiments with similar results were performed. *P* values calculated by *t* test are shown. (**C**) Percentage of LOX-1$^+$ PMN and expression of LOX-1 in PMN isolated from four healthy donors and treated with indicated cytokines. Range of concentrations based on reported data was tested, and only one for each cytokine is shown. Conditioned medium from PCI30 tumor cells (TCM) was used at 20% (v/v) concentration. Means and SD are shown. (**D**) Expression of genes involved in ER stress response in PMN from eight patients with HNC and NSCLC. *P* values calculated by *t* test (for *ATF3* in Mann-Whitney test) are shown. (**E**) Percentage of LOX-1$^+$ PMN and expression of LOX-1 in PMN isolated from four healthy donors and treated with 1 μM THG and 1 mM DTT. Means and SD are shown. *P* values calculated by *t* test are shown.

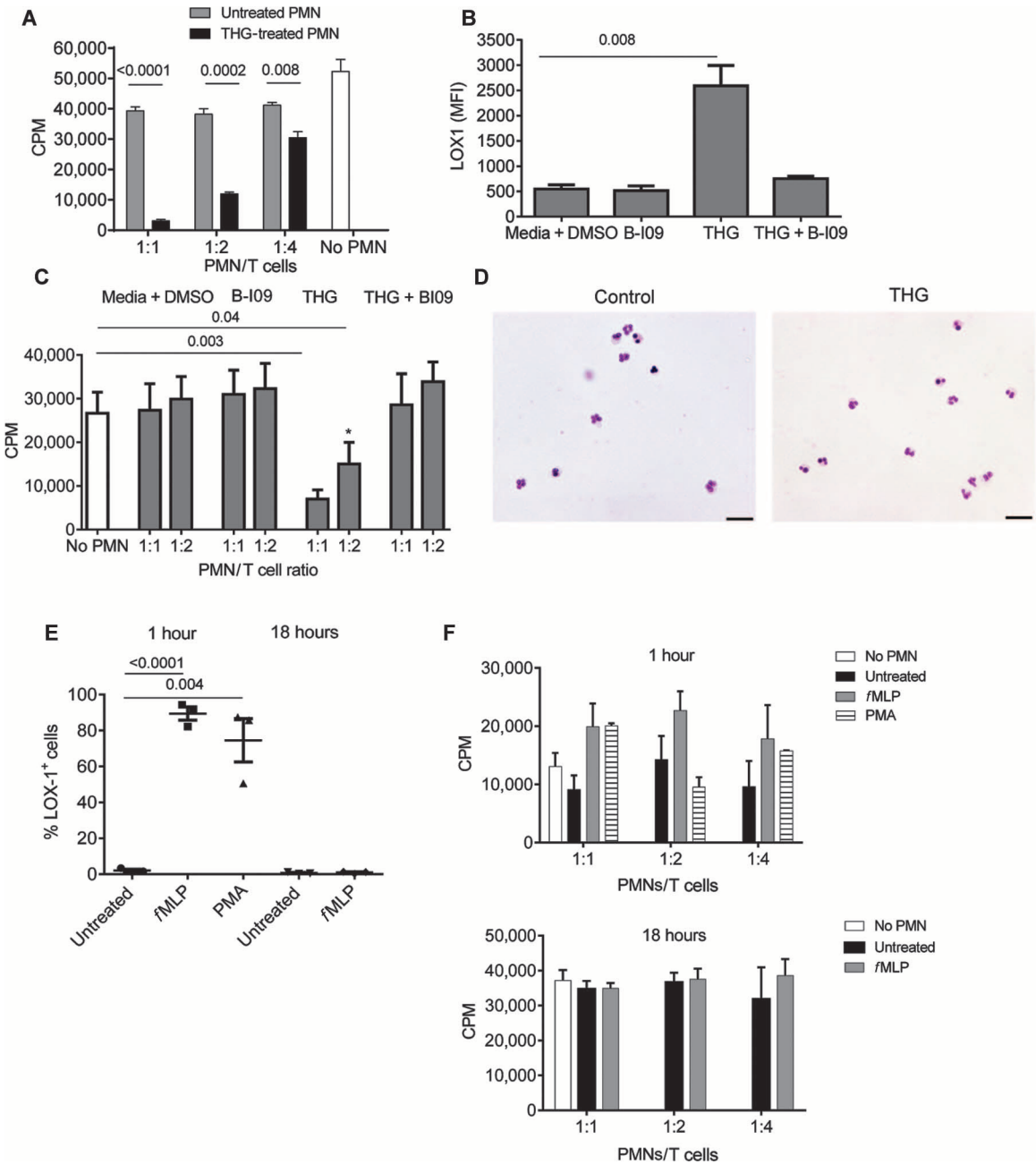

Fig. 5. ER stress induces LOX-1 expression and suppressive activity in PMN. (**A**) The ER stress inducer THG converted PMN to PMN-MDSC. PMNs isolated from healthy donors were treated overnight with 1 μM THG, extensively washed, and then used in CD3/CD28-induced T cell proliferation. T cell proliferation was measured in triplicate by [^{3}H]thymidine uptake. Three experiments with similar results were performed. *P* values calculated by *t* test are shown; $n = 3$. (**B** and **C**) The sXBP1 inhibitor B-I09 abrogated THG-inducible up-regulation of LOX-1 and T cell suppression in PMN from healthy donors. PMNs were incubated together with 20 μM B-I09 and THG overnight followed by evaluation of LOX-1 expression (B) or suppressive activity (C). PMNs from three healthy donors were used in these experiments. *P* values between treated and untreated PMNs (*t* test; $n = 3$). (**D**) Morphology of healthy donor's PMN after 18 hours of incubation with GM-CSF (10 ng/ml) and THG. Giemsa stain. Scale bars, 20 μm. (**E**) Healthy donor's PMNs were cultured for 1 or 18 hours with 10 nM *f*MLP or 20 nM PMA in the presence of GM-CSF (10 ng/ml). The proportion of LOX-1$^+$ cells was evaluated. *P* values were calculated by *t* test ($n = 3$). Analysis of PMA effect after 18 hours was not performed because of undetectable number of viable cells. (**F**) PMNs treated with *f*MLP or PMA as described in (E) were extensively washed after 1 or 18 hours (*f*MLP only) of incubation and tested in a T cell suppression assay. Each experiment was performed in triplicate. Three donors were tested.

LOX-1 defines PMN-MDSC in tumor tissues

It is known that LOX-1 is shed from the surface of the cells and can be detected in plasma (*27*). We evaluated the correlation between the presence of PMN-MDSCs in cancer patients and soluble LOX-1 in plasma. In NSCLC and CC patients, the proportion of PMN-MDSC was associated with soluble LOX-1 (Fig. 6A), suggesting that these cells may be an important source of LOX-1 in plasma of cancer patients.

There is now sufficient evidence demonstrating that tumor MDSCs are more suppressive than cells in PB [reviewed in (*28*)]. We asked whether the population of PMN-MDSCs is more prevalent among all PMNs in tumors than in PB. The proportion of LOX-1$^+$ cells in CD15$^+$ PMN isolated from tumors of patients with HNC and NSCLC was more than threefold higher than in CD15$^+$ PMN from PB of the same patients ($P < 0.001$) (Fig. 6B). Cells in blood and tumor tissues were subjected to the same digestion protocol. However, to exclude possible effect of tissue digestions and isolation on LOX-1 expression, we also evaluated patients with multiple myeloma (MM), where the tumor is located in the BM. We have previously shown a substantial increase of PMN-MDSC in both BM and PB of MM patients (*29*). Similar to solid tumors, the proportion of LOX-1$^+$ PMN-MDSC in BM was three- to fourfold higher than in PB of the same patients ($P = 0.004$) (Fig. 6C). LOX-1$^+$ PMN-MDSC isolated from BM of patients with MM had profound immunosuppressive activity, whereas LOX-1$^-$ PMN did not suppress T cells (Fig. 6D), supporting the conclusion that LOX-1$^+$ PMNs represent PMN-MDSCs at the tumor site.

To evaluate the presence of LOX-1$^+$ PMN-MDSC in tumor tissues, we have developed a method of immunofluorescence staining of paraffin-embedded tissues with the combination of LOX-1 and CD15 antibody (Fig. 6E). Control tissues from normal skin, colon, and lymph nodes had similar low numbers of LOX-1$^+$CD15$^+$ PMN-MDSCs (Fig. 6F). No statistical differences were found in the presence of these cells in melanoma samples, which is consistent with findings that M-MDSCs but not PMN-MDSCs are the predominant population of MDSCs in these patients (*2*). The number of LOX-1$^+$CD15$^+$ PMN-MDSCs in colon carcinoma increased more than 8-fold, in HNC more than 10-fold, and in NSCLC almost 8-fold (Fig. 6F). Thus, LOX-1 expression defines the population of PMN-MDSCs in tumor tissues.

OLR1 expression and the presence of LOX-1$^+$ PMN-MDSC are associated with clinical parameters

Using Oncomine and TCGA (The Cancer Genome Atlas) databases, we evaluated the association of *OLR1* expression in tumor tissues with clinical parameters in different types of cancer. Significant up-regulation of *OLR1* was observed in many types of cancer (Fig. 7A). The notable exception was lung cancer, where normal lung tissues showed markedly higher expression of *OLR1* than did other normal tissues (Fig. 7B), apparently due to cells with high expression of *OLR1* (possibly lung epithelium). *OLR1* expression positively correlated with clinical stage in patients with bladder cancer and clear cell kidney cancer. The positive correlation with tumor size was found in patients with prostate adenocarcinoma, colon adenocarcinoma, bladder cancer, and rectum adenocarcinoma (Fig. 7C). Higher expression of *OLR1* was associated with worse survival in patients with HNC (Fig. 7D). Although these results are suggestive, their interpretation as reflecting the presence of PMN-MDSC has some limitations because of the fact that *OLR1* can be expressed in different cells in the tumor microenvironment. We focused on the evaluation of LOX-1$^+$ PMN-MDSC in tumor tissues and PB.

In patients with NSCLC, we evaluated the possible link between the stage of the disease and the proportion of LOX-1$^+$ PMN-MDSC in PB. Patients with both early (I/II) and late (III/IV) stages of NSCLC had a significantly higher proportion of LOX-1$^+$ PMN-MDSC than healthy donors. There was no statistical significant difference between these two groups of patients (Fig. 7E). However, whereas 85.7% of all patients with late stages of NSCLC had an increase in LOX-1$^+$ PMN-MDSC population, only 50% of patients with early stages showed elevated level of these cells (Fig. 7E). Significant association of the presence of LOX-1$^+$ PMN-MDSC in PB of cancer patients was determined by the size of the tumors. Only patients with large tumors (T2-T3) had significantly higher proportion of LOX-1$^+$ PMN-MDSC than healthy donors, whereas patients with small tumors (T1) had a very low level of LOX-1$^+$ PMN-MDSC similar to healthy donors. Patients with large tumors had significantly more LOX-1$^+$ PMN-MDSC than those with small tumors (Fig. 7F). Using an NSCLC adenocarcinoma tissue array, we evaluated the association between the presence of LOX-1$^+$ PMN-MDSC in tumor tissues and tumor size. Similar to the data obtained in PB, no significant association was found with stage of the disease. The number of LOX-1$^+$ PMN-MDSCs was higher in larger (T2 versus T1) tumors (Fig. 7G).

DISCUSSION

The goal of this study was to address the issue of heterogeneity of human PMN-MDSCs, which limits the progress of our understanding of the biology of these cells. Currently, only partially enriched population of PMN-MDSCs isolated on Ficoll gradient can be evaluated. This population contains not only suppressive PMN-MDSCs but also nonsuppressive activated PMNs. Separation of PMN-MDSCs and PMNs in tumor tissues is not possible, which further complicates the analysis of these cells. Here, we report that PMN-MDSCs have a unique gene expression profile, which is substantially different from that of PMNs from the same patients and from healthy donors. This directly supports the notion that PMN-MDSCs represent a distinct functional state of pathological activation of neutrophils in cancer (*30*, *31*) and is consistent with the analysis of gene expression performed in mice, which demonstrated differences in transcriptome between granulocytes isolated from naïve mice and PMN-MDSCs from tumor-bearing mice (*32*).

Up-regulation of genes associated with ER stress response was a prominent feature of PMN-MDSC. The ER stress response is developed to protect cells from various stress conditions, such as hypoxia, nutrient deprivation, and low pH, and includes three major signaling cascades initiated by three protein sensors: protein kinase RNA-like ER kinase (PERK), inositol-requiring enzyme 1 (IRE1), and ATF6 (*33*). PERK phosphorylates eIF2α, which controls the initiation of mRNA translation and inhibits the flux of synthesized proteins. eIF2α induces the expression of ATF4 and its downstream targets, including the proapoptotic transcription factor CHOP. IRE1 cleaves the mRNA encoding for the transcription factor XBP1 (*34*). sXBP1 mRNA is then ligated by an RNA ligase and translated to produce sXBP1 transcription factor that regulates many target genes including *SEC61a* (*35*).

ER stress response was previously shown to be transmitted to dendritic cells and macrophages from tumor cells and was associated with up-regulation of ARG1 in macrophages (*36*–*38*). Constitutive activation of XBP1 in tumor-associated dendritic cells promoted ovarian cancer progression by blunting antitumor immunity (*39*). We have recently found activation of the ER stress response in MDSC by demonstrating that MDSCs isolated from tumor-bearing mice or cancer patients overexpress sXBP1 and CHOP and displayed an enlarged ER, one of the hallmarks of ER stress (*16*). Another study implicated CHOP in the suppressive activity of MDSC in tumor site (*40*). Consistent with these observations,

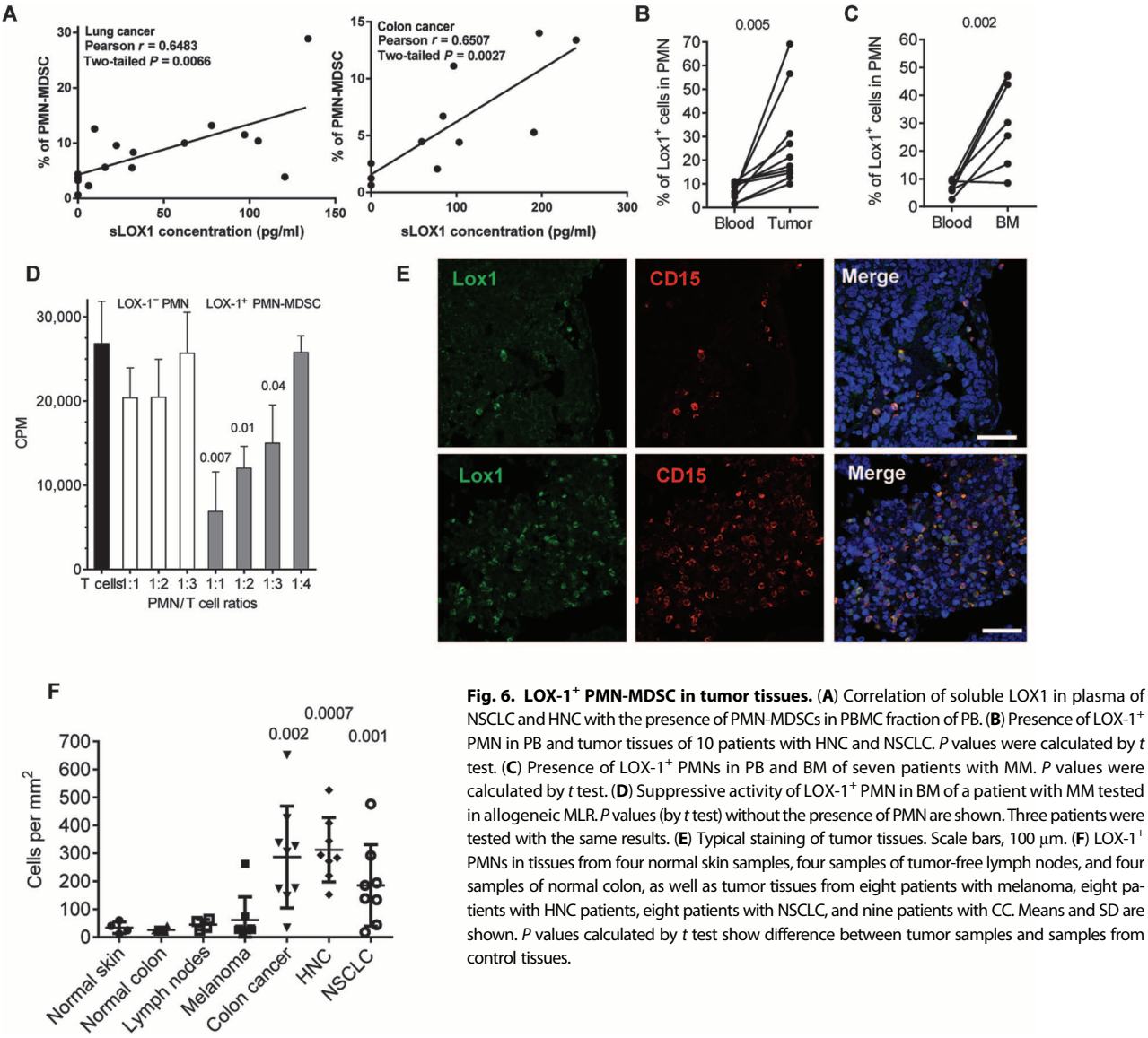

Fig. 6. LOX-1$^+$ PMN-MDSC in tumor tissues. (**A**) Correlation of soluble LOX1 in plasma of NSCLC and HNC with the presence of PMN-MDSCs in PBMC fraction of PB. (**B**) Presence of LOX-1$^+$ PMN in PB and tumor tissues of 10 patients with HNC and NSCLC. *P* values were calculated by *t* test. (**C**) Presence of LOX-1$^+$ PMNs in PB and BM of seven patients with MM. *P* values were calculated by *t* test. (**D**) Suppressive activity of LOX-1$^+$ PMN in BM of a patient with MM tested in allogeneic MLR. *P* values (by *t* test) without the presence of PMN are shown. Three patients were tested with the same results. (**E**) Typical staining of tumor tissues. Scale bars, 100 μm. (**F**) LOX-1$^+$ PMNs in tissues from four normal skin samples, four samples of tumor-free lymph nodes, and four samples of normal colon, as well as tumor tissues from eight patients with melanoma, eight patients with HNC patients, eight patients with NSCLC, and nine patients with CC. Means and SD are shown. *P* values calculated by *t* test show difference between tumor samples and samples from control tissues.

administration of an ER stress inducer to tumor-bearing mice increased the accumulation of MDSCs and their suppressive activity (*41*).

Here, we have determined that the expression of LOX-1 receptor was associated with PMN-MDSCs. LOX-1 is a class E scavenger receptor that is expressed in macrophages and chondrocytes, as well as in endothelial and smooth muscle cells (*20*). The expression of this receptor on neutrophils has not been previously described. We have found that neutrophils from healthy donors and cancer patients have practically undetectable expression of LOX-1. Our data suggested that LOX-1 expression not only is associated with but also defines the population of PMN-MDSC in cancer patients. This conclusion is supported by several lines of evidence: (i) LOX-1$^+$ PMN had gene expression profile similar to that of enriched PMN-MDSC isolated using gradient centrifugation, whereas LOX-1$^-$ PMN had profile similar to neutrophils; (ii) LOX-1$^+$, but not LOX-1$^-$, PMN potently suppressed T cell responses; (iii) LOX-1$^+$ PMN had significantly higher expression of *ARG1* and production of ROS, typical characteristics of PMN-MDSC. We also found that, in tumor tissues, only LOX-1$^+$ PMNs were immunosuppressive and could be considered as PMN-MDSCs. This opens an opportunity for a direct identification of PMN-MDSCs in PB and tumor tissues.

These observations, although unexpected, fit the overall concept of the critical role of ER stress response in MDSC biology. It was recently demonstrated that, in human endothelial cells, oxLDL induced the expression of LOX-1 through activation of the ER stress sensors IRE1 and PERK (*42*). In contrast, ER stress induced by tunicamycin in hepatic L02 cells caused down-regulation of LOX-1. Knockdown of IRE1 or XBP1 restored LOX-1 expression in these cells (*43*). In our experiment, we found that induction of ER stress in neutrophils caused marked up-regulation of LOX-1. This was associated with acquisition of immunosuppressive activity by these cells, indicating that induction of ER stress response could convert neutrophils to PMN-MDSCs. MDSCs accumulate as the result of convergences of two only partially overlapping groups of signals: the signals that promote myelopoiesis (primarily via growth factors and cytokines produced by tumors) and the signals that induce the suppressive activity in these cells (believed to be associated with proinflammatory cytokines) (*17*). ER stress emerged as an

A

Description	TCGA code	Oncomine Up	Oncomine Down	TCGA P	TCGA Fold
Bladder urothelial carcinoma	BLCA			0.0014	4.06
Breast invasive carcinoma	BRCA	13		1E–64	5.22
Cervical and endocervical carcinoma	CESC	1		0.0026	13.74
Colon adenocarcinoma	COAD	5		2E–18	7.12
Glioblastoma multiforme	GBM			0.5334	1.29
Head and neck squamous cell carcinoma	HNSC	2	1	2E–07	2.96
Kidney chromophobe	KICH	1		0.437	1.28
Kidney renal clear cell carcinoma	KIRC	1	1	5E–13	2.73
Kidney renal papillary cell carcinoma	KIRP	1		0.0002	2.4
Liver hepatocellular carcinoma	LIHC			0.661	1.11
Lung adenocarcinoma	LUAD		11	6E–42	–8.08
Lung squamous cell carcinoma	LUSC			1E–54	–16.88
Pancreatic adenocarcinoma	PAAD	1		0.7953	–1.17
Prostate adenocarcinoma	PRAD			8E–05	1.67
Rectum adenocarcinoma	READ			9E–05	6.7
Sarcoma	SARC			0.3766	–2.98
Skin cutaneous melanoma	SKCM			0.6397	–2
Leukemia	na		6	na	na
Gastric cancer	na	1		na	na
Brain	na	1		na	na
All cancers combined	All cancers	na	na	7E–06	1.39

B

	Expression Cancer	Expression Normal	
BLCA	139.1	34.3	Bladder urothelial carcinoma
BRCA	288.8	55.3	Breast invasive carcinoma
CESC	111.6	8.1	Cervical and endocervical carcinoma
COAD	57.8	8.1	Colon adenocarcinoma
GBM	591.4	459.5	Glioblastoma multiforme
HNSC	86.5	29.3	Head and neck squamous cell carcinoma
KICH	99.0	77.1	Kidney chromophobe
KIRC	306.4	112.1	Kidney renal clear cell carcinoma
KIRP	311.5	129.9	Kidney renal papillary cell carcinoma
LIHC	12.4	11.2	Liver hepatocellular carcinoma
LUAD	408.8	3301.5	Lung adenocarcinoma
LUSC	199.7	3370.8	Lung squamous cell carcinoma
PAAD	497.6	582.7	Pancreatic adenocarcinoma
PRAD	47.3	28.3	Prostate adenocarcinoma
READ	49.1	7.3	Rectum adenocarcinoma
SARC	16.9	50.4	Sarcoma
SKCM	41.1	82.3	Skin cutaneous melanoma

C

Stage	Code	Cancer type	*n* patients	*r*, Pearson	*P*
Overall	BLCA	Bladder urothelial carcinoma	252	0.19	0.00293
Overall	KIRC	Kidney renal clear cell carcinoma	519	0.13	0.003868
T	READ	Rectum adenocarcinoma	93	0.33	0.001187
T	BLCA	Bladder urothelial carcinoma	256	0.24	9.17E–05
T	COAD	Colon adenocarcinoma	272	0.18	0.002205
T	PRAD	Prostate adenocarcinoma	361	0.16	0.002056
T	KIRC	Kidney renal clear cell carcinoma	519	0.09	0.032068

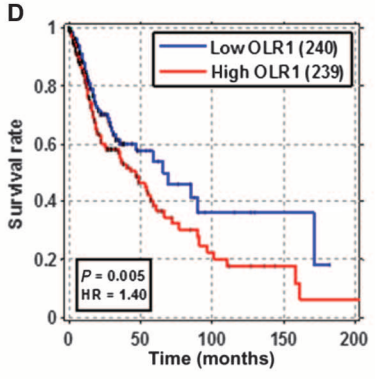

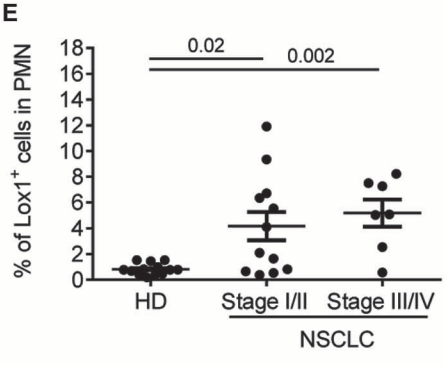

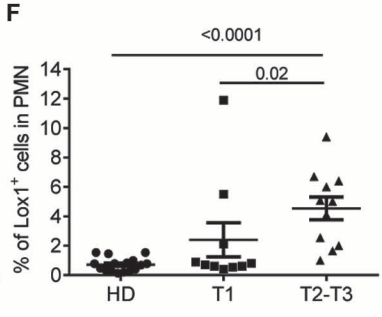

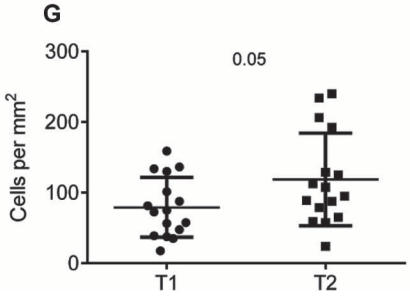

Fig. 7. Clinical association of *OLR1* expression and LOX-1$^+$ PMN-MDSC accumulation in cancer patients. (**A**) Number of independent data sets from Oncomine database that showed *OLR1* up-regulated (up) or down-regulated (down) in cancer versus normal tissues. *P* value and fold change for cancer/normal comparison from TCGA database. na, data not available. (**B**) Average expression values [FPKM (fragments per kilobase of exon per million reads mapped) values] for cancer and normal tissues for different cancers indicate high baseline expression level of *OLR1* in normal lung tissues. (**C**) Association of *OLR1* expression with clinical stage (overall) or tumor size (T) in patients with different types of cancer. (**D**) Kaplan-Meier survival curves for HNC squamous cell carcinoma patients' survival stratified by median *OLR1* expression indicate decreased survival for patients with high *OLR1* expression. *P*, Cox regression *P* value; HR, hazard ratio. (**E**) Proportion of LOX-1$^+$ PMN-MDSC in PB of 12 patients with stage I/II NSCLC, 7 patients with stage III/IV NSCLC, and 16 healthy donors. *P* values were calculated by Mann-Whitney test. (**F**) Proportion of LOX-1$^+$ PMN-MDSC in PB of NSCLC patients segregated on the basis of tumor size. *P* values were calculated by Mann-Whitney test. (**G**) Amount of LOX-1$^+$ CD15$^+$ PMN-MDSC in tumor tissues from NSCLC patients segregated on the basis of tumor size. *P* values were calculated by *t* test.

important factor in the second group. We did not find morphological evidence that PMNs dedifferentiate during the culture with THG. However, in our experiments, we targeted mature neutrophils. It is possible that ER stress may have much broader effect on precursor or progenitor cells.

In our study, we did not investigate whether signaling through LOX-1 is responsible for acquisition of immunosuppressive activity by neutrophils. However, it is likely that it contributes to this process. Engagement of LOX-1 can lead to induction of oxidative stress, apoptosis, and activation of the NF-κB pathway (*18*). These pathways are important for PMN-MDSC function. The ER stress response pathway has been shown to regulate inflammation by activating the NF-κB pathway (*35*, *44*, *45*). LOX-1 up-regulation has been observed during cellular transformation into a cancer cell and can have a pro-oncogenic effect by activating the NF-κB pathway, by increasing DNA damage through increased ROS production, and by promoting angiogenesis and cell dissemination (*46*, *47*). It is possible that LOX-1 signaling may drive pathological activation of PMN toward PMN-MDSC. Cell surface LOX-1 expression can be elevated by multiple stimuli including ROS, inflammatory cytokines [TNF-α and TGF-β (transforming growth factor–β)], and oxLDL (*48*). These factors are produced in cancer, and it is possible that they can affect differentiation of granulocytes from precursors, leading to acquisition of LOX-1 expression. The question is why only 4 to 7% of neutrophils acquire LOX-1 expression and suppressive activity to become PMN-MDSCs. This is an unresolved issue at present mainly because the nature of factors that convert neutrophils to PMN-MDSCs remains unclear. On the basis of mouse studies, it is possible that PMN-MDSCs may have different precursors than most neutrophils, and those precursors are more sensitive to ER stress–inducible factors.

Our study has obvious limitations derived from the nature of human studies and the nature of neutrophils as short-lived differentiated cells. This restrained our ability to provide deeper insight to the mechanism of the observed phenomenon of LOX-1 up-regulation. More information can be generated from the experiments studying progenitors and precursors of neutrophils. For example, we used a neutralizing LOX-1 antibody in an attempt to block signaling through this receptor. This approach may not be sufficient because of the fact that PMN-MDSCs in PB may not be amendable for such regulation. However, LOX-1 can be involved in the regulation of PMN precursors, and the antibody may have an effect. PMN progenitors could be manipulated genetically, which would allow for more precise analysis of this pathway.

We could not find an association between LOX-1 expression and PMN-MDSCs in two mouse models. These results are unexpected, because these models (EL-4 and LLC) are associated with inflammation and expansion of PMN-MDSC. It is possible that such association can be found in other tumor models. However, it is more likely that the expression of LOX-1 in mice and humans is regulated differently. The mechanism remains unclear.

Combination of neutrophil markers with LOX-1 potentially allows for detection of PMN-MDSC in tissues. We observed a marked increase in the number of PMN-MDSC in tumors of patients with HNC, CC, and NSCLC. No such increase was observed in melanoma patients. It is possible that relatively low accumulation of PMN-MDSC in melanoma patients may contribute to this observation. Our data demonstrated that patients have variable amount of LOX-1$^+$ PMN-MDSC, which, at least in patients with NSCLC, was associated with size of the tumors. Further prospective studies are needed to determine whether the presence of these cells in tumor tissues can predict clinical outcome. The expression of LOX-1 on PMN-MDSC opens an opportunity for selective targeting of these cells, because an antibody targeting LOX-1 has already been tested in cardiovascular diseases in mice (*49*, *50*).

MATERIALS AND METHODS

Study design

The aims of this study were to better characterize human PMN-MDSCs and to identify specific markers that allow distinguishing these cells from neutrophils. We performed whole-gene expression array using triplicate of samples. LOX-1 expression was measured by flow cytometry in variable number of replicates indicated in the figure legends. Experiments were performed in a controlled and nonblinded manner. No randomization was performed because of the observational nature of the study. Sample size of patient cohorts was determined on the basis of the results of initial experiments with LOX-1 expression and calculations of expected differences between mean and expected SD.

Human samples

Samples of PB and tumor tissues were collected from patients at the Helen F. Graham Cancer Center and University of Pennsylvania. The study was approved by the institutional review boards (IRBs) of the Christiana Care Health System at the Helen F. Graham Cancer Center, University of Pennsylvania, and Wistar Institute. All patients signed approved consent forms. PB was collected from (i) 26 patients with different stages of NSCLC [12 females, 18 males; ages 59 to 79 years (median, 69 years); 13 patients had squamous cell carcinoma and 13 patients had adenocarcinoma], (ii) 21 patients with HNC [8 females, 13 males; ages 32 to 82 years (median, 65 years); 19 patients had squamous cell carcinoma and 2 patients had adenocarcinoma], (iii) 38 patients with CC (adenocarcinoma) [20 females, 18 males; ages 28 to 88 years (median, 58 years)], and (iv) 6 patients with MM [1 female, 5 males; ages 58 to 81 years (median, 75 years)].

All patients were either previously untreated or received treatment (chemotherapy or radiation therapy) at least 6 months before collection of blood. In some patients, tumor tissues were collected during the surgery. In addition, six patients with eosinophilic colitis, three patients with ulcerative colitis, and eight patients with Crohn's disease were evaluated. Peripheral samples of blood from 18 healthy volunteers [12 females, 6 males; ages 35 to 56 years (median, 42 years)] were used as control. All samples were evaluated within 3 hours after collection.

Lung cancer tumor microarrays were produced from formalin-fixed, paraffin-embedded tissue. Each block was examined by a pathologist; three cores were obtained from tumor-containing areas, and three blocks were from non–tumor-involved lung regions. Samples were obtained from 32 patients with adenocarcinoma. Clinical data obtained included tumor histology, tumor size, disease stage, and time to recurrence (all patients followed for 5 years).

Deidentified samples from normal colonic biopsy colons were obtained from St. Mark's Hospital, Harrow, UK. Samples were taken from patients after obtaining informed consent and with the approval of the Outer West London Research Ethics Committee (UK). Paraffin-embedded tissue blocks of samples of normal skin, lymph nodes, and melanoma were retrieved using an approved IRB protocol for deidentified archived skin biopsies through the Department of Dermatology National Institutes of Health Skin Diseases Research Center Tissue Acquisition Core (P30-AR057217), Perelman School of Medicine, University of Pennsylvania (Philadelphia, PA).

Cell isolation and culture

PMN-MDSC and PMN were isolated by centrifugation over a double-density gradient Histopaque (Sigma) (1.077 to collect PBMCs and 1.119 to collect PMN), labeled with CD15-phycoerythrin (PE) monoclonal antibody (mAb) (BD Biosciences), and then separated using anti-PE beads and MACS column (Miltenyi).

Tissues were first digested with the Tumor Dissociation Kit, human (Miltenyi), and then red blood cells were lysed. Cells were then cultured in RPMI (BioSource International) supplemented with 10% fetal bovine serum, 5 mM glutamine, 25 mM Hepes, 50 μM β-mercaptoethanol, and 1% antibiotics (Invitrogen). In some experiments, recombinant GM-CSF (PeproTech) was added to the culture medium at a concentration of 10 ng/ml.

Isolation of Lox-1$^+$ PMN from PB and suppression assay

Whole blood was enriched for PMNs using MACSxpress Neutrophil Isolation Kit (Miltenyi) following the protocol provided by the manufacturer. Cells were then labeled with anti-Lox1–PE mAb (BioLegend) and then separated using anti-PE beads and MACS column (Miltenyi). For the three-way allogeneic MLR suppression assay, T lymphocytes from one healthy donor were purified with the Human CD3+ T Cell Enrichment Column Kit (R&D Systems) and used as responder cells. Dendritic cells were generated from adherent monocytes from another healthy donor in the presence of GM-CSF (25 ng/ml) and IL-4 (25 ng/ml) (PeproTech) for 6 days and used as stimulator cells. Responder and stimulator cells were then mixed at a 10:1 ratio followed by the addition of Lox1$^+$ or Lox1$^-$ PMNs. T lymphocyte proliferation was assessed after 5 days of culture by thymidine incorporation.

Concurrently, T lymphocytes were isolated from the PBMCs of the same patient as LOX-1$^+$ PMNs using the Human CD3+ T Cell Enrichment Column Kit. PMNs were plated at different ratios with 10^5 T lymphocytes in a 96-well plate coated with anti-CD3 (10 μg/ml) (clone UCHT1; BD Biosciences) followed by the addition of soluble anti-CD28 (1 μg/ml) (clone CD28.2; BD Biosciences). T lymphocyte proliferation was assessed after 3 days of culture by thymidine incorporation. In some experiments, 1 μM NAC (Sigma), 20 μM nor-NOHA (Cayman Chemical), or human LOX-1 mAb (10 μg/ml) (R&D Systems) was added to the culture medium to block ROS or ARG1 activity, respectively. T lymphocyte proliferation was assessed after 5 days of culture by thymidine incorporation.

In vitro PMN Lox-1 induction

PMNs from healthy donors were isolated on a Histopaque gradient. Cells (5×10^5/ml) were cultured for 12 hours with GM-CSF (10 ng/ml) in the presence of DTT (0.5, 1, and 2 mM; Sigma), tunicamycin (0.5, 1, and 2 μg/ml; Sigma-Aldrich), or THG (0.5, 1, and 2 μM; Sigma). In some instances, the XBP1 inhibitor B-I09 (20 μM) was added 3 hours before culture. Cells were then stained for flow cytometry or used for functional assays as described above. For *f*MLP and PMA stimulation, PMNs were isolated from healthy donors and cultured for 1 or 18 hours with either 10 nM *f*MLP (Sigma-Aldrich) or 20 nM PMA (Sigma-Aldrich). Cells were then washed, and LOX1 expression was measured by flow cytometry or used for functional assays as described above. For overnight cultures, GM-CSF (10 ng/ml) was added to the culture.

Flow cytometry

Flow cytometry data were acquired using a BD LSR II flow cytometer and analyzed using FlowJo software (Tree Star).

Immunofluorescence microscopy

After deparaffinization and rehydration, heat-induced antigen retrieval was performed using tris-EDTA buffer (pH 9). Tissues were stained with Lox1 antibody (Abcam, catalog no. ab126538) and CD15 antibody (BD Biosciences, catalog no. 555400) at 1:200 dilution in 5% BSA each for 1 hour at room temperature, followed by blocking with 5% bovine serum albumin (BSA). The following secondary antibodies were used: Alexa Fluor anti-rabbit A647 (1:200 dilution in 5% BSA, Life Technologies) for Lox1 and anti-mouse A514 (1:400 dilution in 5% BSA, Life Technologies) for CD15 staining. CD15 staining was pseudocolored red, and Lox1 staining was pseudocolored green. The nucleus was stained with 4′,6-diamidino-2-phenylindole (1:5000 dilution in phosphate-buffered saline, Life Technologies). Images were obtained using Leica TCS SP5 confocal microscope. Cell counts from 16 frames were used to calculate counts per square millimeter.

Microarray analysis

For sample preparation and hybridization, total RNA from purified cells was isolated with TRIzol reagent according to the manufacturer's recommendations. RNA quality was assessed with the Bioanalyzer (Agilent). Only samples with RNA integrity numbers >8 were used. Equal amount (400 ng) of total RNA was amplified as recommended by Illumina and was hybridized to the Illumina HumanHT-12 v4 human whole-genome bead arrays.

For data preprocessing, the Illumina GenomeStudio software was used to export expression values and calculated detection *P* values for each probe of each sample. Signal intensity data were $\log_2$-transformed and quantile-normalized. Only probes with a significant detection *P* value ($P < 0.05$) in at least one of the samples were considered. The data were submitted to Gene Expression Omnibus (GEO) and are accessible using accession number GSE79404.

Differential expression for probes was tested using "significance analysis of microarrays" method (*51*). Multiple groups were compared using "multiclass" option, and matched patient sample groups were compared using "two-sample paired" option. FDR was estimated using the procedure of Storey and Tibshirani (*52*). Genes with an FDR of <5% were considered significant unless stated otherwise. Hierarchical cluster was performed using standardized Euclidean distance with average linkage. Genes that had Gene Ontology (GO) annotation GO:0005886 (plasma membrane) and either GO:0004872 (receptor activity) or GO:0009897 (external side of plasma membrane) were considered as candidates for surface molecular markers. For expression heat maps, samples from the same patient were additionally normalized to the average between them, and samples from healthy donors were normalized to average between all patient samples. Enrichment analyses were done using IPA (Qiagen, Redwood City; www.qiagen.com/ingenuity). Pathway results with FDR < 5% and $P < 10^{-5}$ were considered significant. Only regulators that passed $P < 10^{-8}$ threshold with significantly predicted ($Z > 2$) activation state in PMN-MDSCs were reported. For OLR1 gene expression associated with cancer, Oncomine (https://www.oncomine.org) was used with "cancer versus normal" gene report without any additional filters. Additionally, TCGA RNA-seqV2 level 3 data (https://tcga-data.nci.nih.gov) were used, and RPKM (reads per kilobase of transcript per million mapped reads) expression values were compared between cancer and normal tissues (where available) using *t* test. Association with survival was done using univariate Cox regression, and Kaplan-Meier curves were plotted for patients split into two groups using median expression. Results with $P < 0.05$ were considered significant.

Quantitative reverse transcription polymerase chain reaction

Total RNA was prepared with E.Z.N.A. Total RNA isolation Kit I (Omega Bio-tek), and complementary DNA (cDNA) was synthesized with High-Capacity cDNA Reverse Transcription Kit (Applied Biosystems). Quantitative reverse transcription PCR was performed with Power SYBR Green PCR Master Mix (Applied Biosystems). The relative amount of mRNA was estimated by the comparative threshold cycle method, with *gapdh* as the reference gene. For the analysis of gene expression, the following primers were used: *sXBP1*, 5′-CTGAGTCCGCAGCAGGTG-3′ and 5′-AGTTGTCCAGAATGCCCAACA-3′; *DDIT3* (*CHOP*), 5′-GCACCTCCCAGAGCCCTCACTCTCC-3′ and 5′-GTCTACTCCAAGCCTTCCCCCTGCG-3′; *ATF4*, 5′-TTCCTGAGCAGCGAGGTGTTG-3′ and 5′-TCCAATCTGTCCCGGAGAAGG-3′; *ATF3*, 5′-TGCCTCGGAAGTGAGTGCTT-3′ and 5′-GCAAAATCCTCAAACACCAGTG-3′; *SEC61a*, 5′-GGATGTATGGGGACCCTTCT-3′ and 5′-CTCGGCCAGTGTTGACAGTA-3′; *ARGI*, 5′-CTTGTTTCGGACTTGCTCGG-3′ and 5′-CACTCTATGTATGGGGGCTTA-3′; *NOS2*, 5′-CAGCGGGATGACTTTCCAA-3′ and 5′-AGGCAAGATTTGGACCTGCA-3′; *GAPDH*, 5′-GGAGTCAACGGATTTGGTCGTA-3′ and 5′-GGCAACAATATCCACTTTACCAGAGT-3′.

Statistics

Statistical analysis was performed using a two-tailed Student's *t* test or Mann-Whitney test after the analysis of distribution of variables. Significance was determined at $P < 0.05$ with normal-based 95% confidence interval means ± 2 SDs. Analysis of gene expression was adjusted for multiple variables, and FDR was estimated as described in (*52*). All calculations were made using GraphPad Prism 5 software (GraphPad Software Inc.).

SUPPLEMENTARY MATERIALS

immunology.sciencemag.org/cgi/content/full/1/2/aaf8943/DC1

Fig. S1. Gene expression differences between PMN-MDSCs and PMNs cells from cancer patients and healthy donors.

Fig. S2. CD16 and LOX-1 staining in PMN.

Fig. S3. Siglec-8 staining of $CD15^+$ PMN.

Fig. S4. LOX1 staining of healthy donor neutrophils.

Fig. S5. List of genes and their relative expression targeted by 93 microarray probes shown to be highly differentially expressed (FDR < 5%, fold > 2) for both $LOX\text{-}1^+/LOX\text{-}1^-$ and PMN-MDSC/PMN comparisons.

Fig. S6. LOX-1 antibody does not induce immunosuppressive activity of PMN.

Fig. S7. LOX-1 expression in mouse PMN-MDSC.

Fig. S8. LOX-1 expression is not associated with mouse PMN-MDSC.

Table S1. Canonical pathways identified by IPA among genes significantly differentially expressed between PMN-MDSC and PMN cells.

Source data (Excel)

REFERENCES AND NOTES

1. T. Condamine, I. Ramachandran, J.-I. Youn, D. I. Gabrilovich, Regulation of tumor metastasis by myeloid-derived suppressor cells. *Annu. Rev. Med.* **66**, 97–110 (2015).
2. M. N. Messmer, C. S. Netherby, D. Banik, S. I. Abrams, Tumor-induced myeloid dysfunction and its implications for cancer immunotherapy. *Cancer Immunol. Immunother.* **64**, 1–13 (2015).
3. J. Finke, J. Ko, B. Rini, P. Rayman, J. Ireland, P. Cohen, MDSC as a mechanism of tumor escape from sunitinib mediated anti-angiogenic therapy. *Int. Immunopharmacol.* **11**, 856–861 (2011).
4. P.-H. Feng, K.-Y. Lee, Y.-L. Chang, Y.-F. Chan, L.-W. Kuo, T.-Y. Lin, F.-T. Chung, C.-S. Kuo, C.-T. Yu, S.-M. Lin, C.-H. Wang, C.-L. Chou, C.-D. Huang, H.-P. Kuo, $CD14^+S100A9^+$ monocytic myeloid-derived suppressor cells and their clinical relevance in non–small cell lung cancer. *Am. J. Respir. Crit. Care Med.* **186**, 1025–1036 (2012).
5. E.-K. Vetsika, F. Koinis, M. Gioulbasani, D. Aggouraki, A. Koutoulaki, E. Skalidaki, D. Mavroudis, V. Georgoulias, A. Kotsakis, A circulating subpopulation of monocytic myeloid-derived suppressor cells as an independent prognostic/predictive factor in untreated non-small lung cancer patients. *J. Immunol. Res.* **2014**, 659294 (2014).
6. C.-Y. Liu, Y.-M. Wang, C.-L. Wang, P.-H. Feng, H.-W. Ko, Y.-H. Liu, Y.-C. Wu, Y. Chu, F.-T. Chung, C.-H. Kuo, K.-Y. Lee, S.-M. Lin, H.-C. Lin, C.-H. Wang, C.-T. Yu, H.-P. Kuo, Population alterations of L-arginase- and inducible nitric oxide synthase-expressed $CD11b^+/CD14^-/CD15^+/CD33^+$ myeloid-derived suppressor cells and $CD8^+$ T lymphocytes in patients with advanced-stage non-small cell lung cancer. *J. Cancer Res. Clin. Oncol.* **136**, 35–45 (2010).
7. C. M. Diaz-Montero, M. L. Salem, M. I. Nishimura, E. Garrett-Mayer, D. J. Cole, A. J. Montero, Increased circulating myeloid-derived suppressor cells correlate with clinical cancer stage, metastatic tumor burden, and doxorubicin–cyclophosphamide chemotherapy. *Cancer Immunol. Immunother.* **58**, 49–59 (2009).
8. C. Meyer, L. Cagnon, C. M. Costa-Nunes, P. Baumgaertner, N. Montandon, L. Leyvraz, O. Michielin, E. Romano, D. E. Speiser, Frequencies of circulating MDSC correlate with clinical outcome of melanoma patients treated with ipilimumab. *Cancer Immunol. Immunother.* **63**, 247–257 (2014).
9. A. A. Tarhini, H. Edington, L. H. Butterfield, Y. Lin, Y. Shuai, H. Tawbi, C. Sander, Y. Yin, M. Holtzman, J. Johnson, U. N. M. Rao, J. M. Kirkwood, Immune monitoring of the circulation and the tumor microenvironment in patients with regionally advanced melanoma receiving neoadjuvant ipilimumab. *PLOS One* **9**, e87705 (2014).
10. Z. Wang, Y. Zhang, Y. Liu, L. Wang, L. Zhao, T. Yang, C. He, Y. Song, Q. Gao, Association of myeloid-derived suppressor cells and efficacy of cytokine-induced killer cell immunotherapy in metastatic renal cell carcinoma patients. *J. Immunother.* **37**, 43–50 (2014).
11. S. E. Finkelstein, T. Carey, I. Fricke, D. Yu, D. Goetz, M. Gratz, M. Dunn, P. Urbas, A. Daud, R. DeConti, S. Antonia, D. Gabrilovich, M. Fishman, Changes in dendritic cell phenotype after a new high-dose weekly schedule of interleukin-2 therapy for kidney cancer and melanoma. *J. Immunother.* **33**, 817–827 (2010).
12. T. Kimura, J. R. McKolanis, L. A. Dzubinski, K. Islam, D. M. Potter, A. M. Salazar, R. E. Schoen, O. J. Finn, MUC1 vaccine for individuals with advanced adenoma of the colon: A cancer immunoprevention feasibility study. *Cancer Prev. Res.* **6**, 18–26 (2013).
13. J.-I. Youn, S. Nagaraj, M. Collazo, D. I. Gabrilovich, Subsets of myeloid-derived suppressor cells in tumor-bearing mice. *J. Immunol.* **181**, 5791–5802 (2008).
14. I. Poschke, R. Kiessling, On the armament and appearances of human myeloid-derived suppressor cells. *Clin. Immunol.* **144**, 250–268 (2012).
15. S. Mandruzzato, S. Brandau, C. M. Britten, V. Bronte, V. Damuzzo, C. Gouttefangeas, D. Maurer, C. Ottensmeier, S. H. van der Burg, M. J. P. Welters, S. Walter, Toward harmonized phenotyping of human myeloid-derived suppressor cells by flow cytometry: Results from an interim study. *Cancer Immunol. Immunother.* **65**, 161–169 (2016).
16. T. Condamine, V. Kumar, I. R. Ramachandran, J.-I. Youn, E. Celis, N. Finnberg, W. S. El-Deiry, R. Winograd, R. H. Vonderheide, N. R. English, S. C. Knight, H. Yagita, J. C. McCaffrey, S. Antonia, N. Hockstein, R. Witt, G. Masters, T. Bauer, D. I. Gabrilovich, ER stress regulates myeloid-derived suppressor cell fate through TRAIL-R–mediated apoptosis. *J. Clin. Invest.* **124**, 2626–2639 (2014).
17. T. Condamine, J. Mastio, D. I. Gabrilovich, Transcriptional regulation of myeloid-derived suppressor cells. *J. Leukoc. Biol.* **98**, 913–922 (2015).
18. N. Al-Banna, C. Lehmann, Oxidized LDL and LOX-1 in experimental sepsis. *Mediators Inflamm.* 2013, 761789 (**2013**).
19. T. Sawamura, N. Kume, T. Aoyama, H. Moriwaki, H. Hoshikawa, Y. Aiba, T. Tanaka, S. Miwa, Y. Katsura, T. Kita, T. Masaki, An endothelial receptor for oxidized low-density lipoprotein. *Nature* **386**, 73–77 (1997).
20. A. Taye, A. A. K. El-Sheikh, Lectin-like oxidized low-density lipoprotein receptor 1 pathways. *Eur. J. Clin. Invest.* **43**, 740–745 (2013).
21. R. Yoshimoto, Y. Fujita, A. Kakino, S. Iwamoto, T. Takaya, T. Sawamura, The discovery of LOX-1, its ligands and clinical significance. *Cardiovasc. Drugs Ther.* **25**, 379–391 (2011).
22. I. Moldovan, J. Galon, I. Maridonneau-Parini, S. Roman Roman, C. Mathiot, W.-H. Fridman, C. Sautès-Fridman, Regulation of production of soluble Fcγ receptors type III in normal and pathological conditions. *Immunol. Lett.* **68**, 125–134 (1999).
23. A. Banerjee, N. K. Mondal, D. Das, M. R. Ray, Neutrophilic inflammatory response and oxidative stress in premenopausal women chronically exposed to indoor air pollution from biomass burning. *Inflammation* **35**, 671–683 (2012).
24. J. L. Mehta, N. Sanada, C. P. Hu, J. Chen, A. Dandapat, F. Sugawara, H. Satoh, K. Inoue, Y. Kawase, K.-i. Jishage, H. Suzuki, M. Takeya, L. Schnackenberg, R. Beger, P. L. Hermonat, M. Thomas, T. Sawamura, Deletion of LOX-1 reduces atherogenesis in LDLR knockout mice fed high cholesterol diet. *Circ. Res.* **100**, 1634–1642 (2007).
25. A. Pirillo, G. D. Norata, A. L. Catapano, LOX-1, OxLDL, and atherosclerosis. *Mediators Inflamm.* **2013**, 152786 (2013).
26. C.-H. A. Tang, S. Ranatunga, C. L. Kriss, C. L. Cubitt, J. Tao, J. A. Pinilla-Ibarz, J. R. Del Valle, C.-C. Hu, Inhibition of ER stress-associated IRE-1/XBP-1 pathway reduces leukemic cell survival. *J. Clin. Invest.* **124**, 2585–2598 (2014).
27. T. Sawamura, A. Kakino, Y. Fujita, LOX-1: A multiligand receptor at the crossroads of response to danger signals. *Curr. Opin. Lipidol.* **23**, 439–445 (2012).

28. V. Kumar, S. Patel, E. Tcyganov, D. Gabrilovich, The nature of myeloid-derived suppressor cells in the tumor microenvironment. *Trends Immunol.* **37**, 208–220 (2016).
29. I. R. Ramachandran, A. Martner, A. Pisklakova, T. Condamine, T. Chase, T. Vogl, J. Roth, D. Gabrilovich, Y. Nefedova, Myeloid-derived suppressor cells regulate growth of multiple myeloma by inhibiting T cells in bone marrow. *J. Immunol.* **190**, 3815–3823 (2013).
30. D. I. Gabrilovich, S. Ostrand-Rosenberg, V. Bronte, Coordinated regulation of myeloid cells by tumours. *Nat. Rev. Immunol.* **12**, 253–268 (2012).
31. D. Marvel, D. I. Gabrilovich, Myeloid-derived suppressor cells in the tumor microenvironment: Expect the unexpected. *J. Clin. Invest.* **125**, 3356–3364 (2015).
32. Z. G. Fridlender, J. Sun, I. Mishalian, S. Singhal, G. Cheng, V. Kapoor, W. Horng, G. Fridlender, R. Bayuh, G. S. Worthen, S. M. Albelda, Transcriptomic analysis comparing tumor-associated neutrophils with granulocytic myeloid-derived suppressor cells and normal neutrophils. *PLOS One* **7**, e31524 (2012).
33. M. Holcik, N. Sonenberg, Translational control in stress and apoptosis. *Nat. Rev. Mol. Cell Biol.* **6**, 318–327 (2005).
34. D. Ron, P. Walter, Signal integration in the endoplasmic reticulum unfolded protein response. *Nat. Rev. Mol. Cell Biol.* **8**, 519–529 (2007).
35. N. Cláudio, A. Dalet, E. Gatti, P. Pierre, Mapping the crossroads of immune activation and cellular stress response pathways. *EMBO J.* **32**, 1214–1224 (2013).
36. N. R. Mahadevan, V. Anufreichik, J. J. Rodvold, K. T. Chiu, H. Sepulveda, M. Zanetti, Cell-extrinsic effects of tumor ER stress imprint myeloid dendritic cells and impair $CD8^+$ T cell priming. *PLOS One* **7**, e51845 (2012).
37. N. R. Mahadevan, J. Rodvold, H. Sepulveda, S. Rossi, A. F. Drew, M. Zanetti, Transmission of endoplasmic reticulum stress and pro-inflammation from tumor cells to myeloid cells. *Proc. Natl. Acad. Sci. U.S.A.* **108**, 6561–6566 (2011).
38. N. R. Mahadevan, M. Zanetti, Tumor stress inside out: Cell-extrinsic effects of the unfolded protein response in tumor cells modulate the immunological landscape of the tumor microenvironment. *J. Immunol.* **187**, 4403–4409 (2011).
39. P. Walter, D. Ron, The unfolded protein response: From stress pathway to homeostatic regulation. *Science* **334**, 1081–1086 (2011).
40. P. T. Thevenot, R. A. Sierra, P. L. Raber, A. A. Al-Khami, J. Trillo-Tinoco, P. Zarreii, A. C. Ochoa, Y. Cui, L. Del Valle, P. C. Rodriguez, The stress-response sensor chop regulates the function and accumulation of myeloid-derived suppressor cells in tumors. *Immunity* **41**, 389–401 (2014).
41. B. R. Lee, S. Y. Chang, E. H. Hong, B. E. Kwon, H. M. Kim, Y. J. Kim, J. Lee, H. J. Cho, J. H. Cheon, H. J. Ko, Elevated endoplasmic reticulum stress reinforced immunosuppression in the tumor microenvironment via myeloid-derived suppressor cells. *Oncotarget* **5**, 12331–12345 (2014).
42. D. Hong, Y. P. Bai, H. C. Gao, X. Wang, L. F. Li, G. G. Zhang, C. P. Hu, Ox-LDL induces endothelial cell apoptosis via the LOX-1-dependent endoplasmic reticulum stress pathway. *Atherosclerosis* **235**, 310–317 (2014).
43. D. Hong, L. F. Li, H. C. Gao, X. Wang, C. C. Li, Y. Luo, Y. P. Bai, G. G. Zhang, High-density lipoprotein prevents endoplasmic reticulum stress-induced downregulation of liver LOX-1 expression. *PLOS One* **10**, e0124285 (2015).
44. S. E. Bettigole, L. H. Glimcher, Endoplasmic reticulum stress in immunity. *Annu. Rev. Immunol.* **33**, 107–138 (2014).
45. K. Zhang, R. J. Kaufman, From endoplasmic-reticulum stress to the inflammatory response. *Nature* **454**, 455–462 (2008).
46. H. A. Hirsch, D. Iliopoulos, A. Joshi, Y. Zhang, S. A. Jaeger, M. Bulyk, P. N. Tsichlis, X. Shirley Liu, K. Struhl, A transcriptional signature and common gene networks link cancer with lipid metabolism and diverse human diseases. *Cancer Cell* **17**, 348–361 (2010).
47. J. Lu, S. Mitra, X. Wang, M. Khaidakov, J. L. Mehta, Oxidative stress and lectin-like ox-LDL-receptor LOX-1 in atherogenesis and tumorigenesis. *Antioxid. Redox Signal.* **15**, 2301–2333 (2011).
48. X. Wang, M. I. Phillips, J. L. Mehta, LOX-1 and angiotensin receptors, and their interplay. *Cardiovasc. Drugs Ther.* **25**, 401–417 (2011).
49. J. De Siqueira, I. Abdul Zani, D. A. Russell, S. B. Wheatcroft, S. Ponnambalam, S. Homer-Vanniasinkam, Clinical and preclinical use of LOX-1-specific antibodies in diagnostics and therapeutics. *J. Cardiovasc. Transl. Res.* **8**, 458–465 (2015).
50. J. L. Mehta, M. Khaidakov, P. L. Hermonat, S. Mitra, X. Wang, G. Novelli, T. Sawamura, LOX-1: A new target for therapy for cardiovascular diseases. *Cardiovasc. Drugs Ther.* **25**, 495–500 (2011).
51. S. Zhang, A comprehensive evaluation of SAM, the SAM R-package and a simple modification to improve its performance. *BMC Bioinformatics* **8**, 230 (2007).
52. J. D. Storey, R. Tibshirani, Statistical significance for genomewide studies. *Proc. Natl. Acad. Sci. U.S.A.* **100**, 9440–9445 (2003).

Acknowledgments: We thank Q. Liu for help with statistical analysis and C. C. Hu and J. R. Del Valle for providing us with B-I09 inhibitor. **Funding:** This work was supported in part by the NIH (grants CA084488 and CA100062) and Janssen Pharmaceutical to D.I.G., the National Cancer Institute (grant P01 CA 098101) and American Cancer Society (grant RP-10-033-01-CCE) to A.R., and the flow cytometry and bioinformatics core facilities at the Wistar Institute. **Author contributions:** T.C. designed and performed most of the experiments and analyzed data; G.A.D. performed experiments, analyzed data, and wrote the manuscript; J.-I.Y., S.M., K.A.-T., E.T., A.H., C.L., and S.P. performed experiments; A.V.K. performed bioinformatics analysis; Y.N. analyzed data and wrote the manuscript; A.G., D.T.V., X.X., S.C.K., G. Malietzis, G.H.L., E.E., S.M.A., M.B., A.R., N.H., R.W., G. Masters, and B.N. provided clinical material and analyzed clinical correlates; X.W. and J.L.M. provided LOX-$1^{-/-}$ BM for the experiment; D.S. and M.A.S. designed experiments and analyzed data; D.I.G. designed the concept of the study and experiments, analyzed data, and wrote the manuscript. **Competing interests:** The authors declare that they have no competing interests. **Data and materials availability:** The data for this study have been deposited to GEO database and are accessible using accession number GSE79404.

Submitted 20 April 2016
Accepted 12 July 2016
Published 5 August 2016
10.1126/sciimmunol.aaf8943

Citation: T. Condamine, G. A. Dominguez, J.-I. Youn, A. V. Kossenkov, S. Mony, K. Alicea-Torres, E. Tcyganov, A. Hashimoto, Y. Nefedova, C. Lin, S. Partlova, A. Garfall, D. T. Vogl, X. Xu, S. C. Knight, G. Malietzis, G. H. Lee, E. Eruslanov, S. M. Albelda, X. Wang, J. L. Mehta, M. Bewtra, A. Rustgi, N. Hockstein, R. Witt, G. Masters, B. Nam, D. Smirnov, M. A. Sepulveda, D. I. Gabrilovich, Lectin-type oxidized LDL receptor-1 distinguishes population of human polymorphonuclear myeloid-derived suppressor cells in cancer patients. *Sci. Immunol.* **1**, aaf8943 (2016).

Science Immunology
AAAS

Lectin-type oxidized LDL receptor-1 distinguishes population of human polymorphonuclear myeloid-derived suppressor cells in cancer patients

Thomas Condamine, George A. Dominguez, Je-In Youn, Andrew V. Kossenkov, Sridevi Mony, Kevin Alicea-Torres, Evgenii Tcyganov, Ayumi Hashimoto, Yulia Nefedova, Cindy Lin, Simona Partlova, Alfred Garfall, Dan T. Vogl, Xiaowei Xu, Stella C. Knight, George Malietzis, Gui Han Lee, Evgeniy Eruslanov, Steven M. Albelda, Xianwei Wang, Jawahar L. Mehta, Meenakshi Bewtra, Anil Rustgi, Neil Hockstein, Robert Witt, Gregory Masters, Brian Nam, Denis Smirnov, Manuel A. Sepulveda and Dmitry I. Gabrilovich

*Sci. Immunol.*1, aaf8943 (2016)
doi: 10.1126/sciimmunol.aaf8943

Editor's Summary Stressing myeloid-derived suppressor cells in cancerImmunotherapies for cancer have shown promising results in part because they overcome the suppressive effects of the tumor microenvironment on immune cells. Condamine et al. now report that polymorphonuclear myeloid-derived suppressor cells (PMN-MDSCs) can be distinguished from neutrophils in the same cancer patient by the expression of the lipid metabolism-related molecule lectin-type oxidized LDL receptor-1 (LOX-1). LOX-1-expressing neutrophils were nearly undetectable in healthy individuals but were found prominently in tumor tissues. Moreover, exposing neutrophils from healthy individuals to endoplasmic reticulum stress resulted in up-regulation of LOX-1 and increased suppressive function. These data support the specific targeting of LOX-1-expressing PMN-MDSC for cancer immunotherapy.

Science Immunology (ISSN 2375-2548) publishes new articles weekly. The journal is published by the American Association for the Advancement of Science (AAAS), 1200 New York Avenue NW, Washington, DC 20005.